https://doi.org/10.5194/acp-2019-969
Preprint. Discussion started: 23 January 2020


Atmospheric Chemistry and Physics Discussions

# Development and application of the WRFDA-Chem 3DVAR system: aiming to improve air quality forecast and diagnose model deficiencies

Wei Sun[1,2], Zhiquan Liu[1*], Dan Chen[3*], Pusheng Zhao[3], and Min Chen[3]

[1] National Center for Atmospheric Research, Boulder, CO, 80301, USA

[2] National Space Science Center, Chinese Academy of Sciences, Beijing, 100190, China

[3] Institute of Urban Meteorology, China Meteorology Administration, Beijing, 100089, China

* *Corresponding author: Dr. Zhiquan Liu (liuz@ucar.edu) and Dr. Dan Chen (dchen@ium.cn)*

https://doi.org/10.5194/acp-2019-969
Preprint. Discussion started: 23 January 2020


Atmospheric Chemistry and Physics Discussions


## Abstract

To improve the operational air quality forecasting over China, a new aerosol/gas phase pollutants assimilation capability is developed within the WRFDA system using 3DVAR algorithm. In this first application, the interface for MOSAIC aerosol scheme is built with flexible extending potentials. Based on the new WRFDA-Chem system, five experiments assimilating different surface observations, including $PM_{2.5}$, $PM_{10}$, $SO_2$, $NO_2$, $O_3$, and CO are conducted for January 2017 along with a control experiment without DA. Results exhibit that the WRFDA-Chem system evidently improves the air quality forecasting. On the analysis aspect, the assimilation of surface observations reduces the bias and RMSE in the initial condition (IC) remarkably; on the forecast aspect, better forecast performances are acquired up to 24-h, in which the experiment assimilating the six pollutants simultaneously displays the best forecast skill overall. With respect to the impact of DA cycling frequency, the responses toward IC updating are found out to be different among the pollutants. For $PM_{2.5}$, $PM_{10}$, $SO_2$ and CO, the forecast skills increase with the DA frequency; for $O_3$, although improvements are acquired at the 6-h cycling frequency, the advantage of more frequent DA could be consumed by the disadvantage of unbalanced photochemistry (due to inaccurate precursor NOx/VOC ratios) from assimilating the existing observations (only $O_3$ and $NO_2$, but no VOC). Considering after one aspect (IC) in the model is corrected by DA, the deficiencies from other aspects (e.g., chemical reactions) could be more evident, this study further explores the model deficiencies by investigating the effects of assimilating gaseous precursors on the forecast of related aerosols. Results exhibit that the parameterization (uptake coefficients) in the newly added Sulfate-Nitrate-Ammonium (SNA) relevant heterogeneous reactions in the model are not fully appropriate although it best simulates observed SNA aerosols without DA; since the uptake coefficients were originally tuned under the inaccurate gaseous precursor scenarios

https://doi.org/10.5194/acp-2019-969
Preprint. Discussion started: 23 January 2020


Atmospheric Chemistry and Physics Discussions

without DA, the biases from the two aspects (SNA reactions and IC DA) were just compensated. In the future chemistry development, parameterizations (such as uptake coefficients) for different gaseous precursor scenarios should be adjusted and verified with the help of DA technique. According to these results, DA ameliorates certain aspects by using observation as constraints, and thus provides an opportunity to identify and diagnose the model deficiencies; it is useful especially when the uncertainties of various aspects are mixed up and the reaction paths are not clearly revealed. In the future, besides being used to improve the forecast through updating IC, DA could be treated as another approach to explore necessary developments in the model.

## 1. Introduction

Air pollution is almost inevitable for all developed (historically) and developing (in present days) countries. From acid rain, haze to smog etc., the air pollution significantly impacts atmospheric visibility, human health, and climate. As one of the fastest growing countries, China has been suffering from extreme haze with high particulate matter (PM) national-wide and increasing tropospheric ozone ($O_3$) pollution in city clusters (Fu et al., 2019; Lu et al., 2019). To control the pollutions as well as to improve the air quality forecast, Chinese governments had enforced stricter air quality standards from 2012, and deployed monitoring network for six "criteria" air pollutants since 2013, which includes $PM_{2.5}$ and $PM_{10}$ (aerosols/fine particulate matter with aerodynamic diameters less than 2.5 or 10 $\mu$m), $SO_2$ (sulfur dioxide), $NO_2$ (nitrogen dioxide), $O_3$ (ozone), and CO (carbon monoxide). Among the six pollutants, the forecast on aerosols (especially $PM_{2.5}$) is of greatest research interest as the severity of aerosol pollution and its negative effects on both health and climate. However, it's still challenging to accurately simulate and forecast aerosols by pure air quality models due to some issues, such as the

https://doi.org/10.5194/acp-2019-969
Preprint. Discussion started: 23 January 2020


Atmospheric Chemistry and Physics Discussions

large uncertainties in primary and precursor emissions processes, the incomplete understanding and parameterization of secondary inorganic/organic reactions from precursors, and the accumulation of meteorology simulation errors. In addition to aerosol forecast, the elevated $O_3$ levels in city clusters over eastern China draw more and more attentions recently. Under this circumstance, in the urban regions in China, where suffer from complex air pollution with both haze and smog, the accurate forecast of air quality has been not only a challenge for operational centers, but also a common concern for scientific community.

To improve the forecast skill, data assimilation (DA), a combination of observations and numerical model output, has been widely used in meteorology forecast since last century, and recently extended to air pollutant forecasts. Based upon various techniques, DA is proven to be skillful at improving the meteorology and aerosol forecasts (Bannister 2017; McHenry et al. 2015; Peng et al. 2018; Sandu and Chai 2011; Schutgens et al. 2010; Sekiyama et al. 2010; Tang et al. 2011; Tang et al. 2013). Focusing on aerosol assimilation, NCAR group had conducted a series of work. Using three-dimensional variational (3DVAR) algorithm, Liu et al. (2011) implemented DA on aerosol optical depth estimates within the Grid-point Statistical Interpolation (GSI) system. Schwartz et al. (2012), Jiang et al. (2013), and Chen et al. (2019) further extended this system to assimilate surface $PM_{2.5}$ and $PM_{10}$. It should be noted that the aerosols are complicated not merely from primary emissions but also secondary reactions with gaseous precursors in the atmosphere (Huang et al. 2014; Nie et al. 2014; Xie et al. 2015). However, the assimilation of aerosols along with gas phase pollutants are seldom investigated. Recently, it is encouraging that an Ensemble Kalman Filter (EnKF) DA system is developed to assimilate multi-species surface chemical observations (Peng et al. 2017), while the EnKF system may not be the favorite choice in operational applications due to its massive computational cost. In addition,

https://doi.org/10.5194/acp-2019-969
Preprint. Discussion started: 23 January 2020


Atmospheric Chemistry and Physics Discussions

74 at the Institute of Urban Meteorology (IUM), regional NWP system–RMAPS-ST (adapted from WRF)
75 and regional air quality model–RMAPS-Chem (adapted from WRF-Chem) are applied operationally
76 for the weather and air quality forecast over Northern China. RMAPS-ST provides the meteorology
77 drivers for RMAPS-Chem, and WRFDA is utilized for the meteorology DA in RMAPS-ST (Fan et al.
78 2016; Yu et al. 2018). In result, to implement the assimilations of aerosols along with gas phase
79 pollutants in the future air quality forecast operational system (e.g. the RMPAS-Chem), and to design
80 an efficient and unified DA platform that satisfies the operational needs in both meteorology and air
81 quality forecast, this study works on the WRFDA system with 3DVAR algorithm. To the authors'
82 knowledge, this is the first attempt to assimilate hourly ground-based aerosols simultaneously with gas
83 phase pollutants in the WRFDA system.

84 With regard to the aerosol data assimilation, the first and foremost challenge comes from the
85 complex components related to the aerosol scheme. With different emphasis and applications, the
86 chosen aerosol scheme in the model could be different, which will lead to various choices and
87 treatment for the analysis variables in the DA system. For example, in the existed DA developments,
88 many studies used the GOCART aerosol scheme to address the dust or the natural-source related events.
89 However, the GOCART aerosol scheme is well known to underestimate the PM concentrations due to
90 lack of secondary organic aerosol (SOA) formation, as well as aerosol species related to the
91 anthropogenic emission, such as nitrate and ammonium (McKeen et al. 2009; Pang et al. 2018).
92 Different from the GOCART scheme, the MOSAIC (Model for Simulating Aerosol Interactions and
93 Chemistry) aerosol scheme uses a sectional approach to represent the aerosol size distribution with
94 different size bins, and it takes black carbon, organic carbon, sulfate, nitrate, ammonium, sodium,
95 chloride, and other inorganic compounds that are related to anthropogenic emissions into consideration.

https://doi.org/10.5194/acp-2019-969
Preprint. Discussion started: 23 January 2020


Atmospheric Chemistry and Physics Discussions

96 In result, the MOSAIC scheme exhibits a better performance in representing the complex $PM_{2.5}$
97 pollution over China (Chen et al. 2016; Chen et al. 2019). Therefore, to make the DA system suitable
98 for different emphasis and applications, a flexible aerosol assimilation capability is built within the
99 WRFDA system in this study, which will facilitate developments and applications for more chemistry
100 schemes in the future. Focusing on the air quality forecast over China, this study mainly analyses the
101 results of MOSAIC aerosol scheme.

102 It should be mentioned that the forecast performance with data assimilation also relies on the air
103 quality model itself. Due to the limited observational information as constraint, the DA system uses
104 large parts of model mechanism and processes to derive the full analysis information (e.g. use total
105 PM mass observations to analyze all PM components). However, there are still potential deficiencies
106 in the model. For example, some reaction paths are missing in the heavily polluted events in China
107 (e.g. Wang et al., 2014), since the chemistry schemes are originally developed for relatively clean areas
108 and recent observed pathways haven't been timely reflected in the model. Moreover, the large
109 uncertainties of precursor and primary emissions could bring errors to the aerosol species partitioning
110 and size distribution in the model. Nevertheless, when it comes to DA, as one aspect (initial conditions
111 of aerosols and some precursors) in the model is corrected by using observation as constraints, the
112 deficiencies from other aspects, such as the above mentioned chemical reactions, could be more
113 evident. From this point of view, after investigating to what extend the DA technique can help to
114 improve the forecast of air quality, this study further explores the model deficiencies with the help of
115 DA, aiming to provide helpful indications for future model development.

116 In the rest of the paper, an overview of the model description, observations and methodology is
117 presented in Section 2, followed by evaluations of the new WRFDA-Chem system in Section 3.

https://doi.org/10.5194/acp-2019-969
Preprint. Discussion started: 23 January 2020


Atmospheric Chemistry and Physics Discussions

118 Section 4 analyzes the DA experiments in consideration of potential issues in the model, aiming to
119 provide beneficial references on further model development. Conclusions and discussions are given in
120 section 5.

121 **2. Model description, observations and methodology**

122 In this study, the interfaced air quality model is WRF-Chem. The WRF-Chem settings are very
123 similar to those of Chen et al. (2016). Here, only a brief summary of the model configuration and
124 observations is provided below. Descriptions of the most important development of this study, the
125 WRFDA-Chem system, are presented in Section 2.3.

126 **2.1 WRF-Chem model and emissions**

127 As in Chen et al. (2016), version 3.6.1 of the WRF-Chem model is used in this study to simulate
128 the aerosols and gas-phase chemistry processes. A summary of the used physical parameterizations is
129 given in Table 1. Details of the WRF-Chem model have been described by Grell et al. (2005) and Fast
130 et al. (2006). The Carbon Bond Mechanism version Z (CBMZ) and Model for Simulating Aerosol
131 Interactions and Chemistry (MOSAIC) schemes are used as the gas-phase and aerosol chemical
132 mechanisms, respectively. The relative humidity (RH) dependent heterogeneous reactions added by
133 Chen et al. (2016) are also applied in the simulations. The model computational domain covers most
134 of China and its surrounding regions. Figure 1 presents the horizontal range of the domain, which
135 contains 121 x 121 horizontal grids at a 40.5-km resolution. Vertically, there are 57 levels extending
136 from the surface to 10 hPa.

https://doi.org/10.5194/acp-2019-969
Preprint. Discussion started: 23 January 2020


Atmospheric Chemistry and Physics Discussions

As in Chen et al. (2019), the emission input is based on the 2010 Multi-resolution Emission Inventory for China (MEIC) (He 2012; Lei et al. 2011; Li et al. 2014; Zhang et al. 2009), which has already been applied in many recent studies over China (Wang et al. 2016; Wang et al. 2013; Zheng et al. 2015). The emission inventory has also been processed to match the model grid spacing (40.5 km) from an original grid spacing of 0.25° × 0.25° (Chen et al. 2016). Admittedly, the difference between the emission base year and our simulation year and the spatial-temporal allocations may arise uncertainties in our simulation, this emission is the only publicly available emission inventory when the study is conducted. Meanwhile, the inhomogeneous spatial changes and large uncertainties in seasonal allocations of the emissions made it difficult to simply scale the original emission inventory for our study period (Chen et al. 2019).

### 2.2 Observations

For the future application in RMAPS-Chem operational air quality forecast system, the WRFDA-Chem system is designed to assimilate the hourly surface observations of six major pollutants ($PM_{2.5}$, $PM_{10}$, $SO_2$, $NO_2$, $O_3$, and CO) from the China National Environmental Monitoring Center (CNEMC). To verify capability of the system, we use the data for the whole month of January 2017. As in Chen et al. (2019), to perform statistical calculations, an observation dataset at 531 locations (Fig. 1) is acquired by averaging all the original observations (1600+ sites) that fall into the same model grid. Meanwhile, two steps of data quality control are conducted before DA. Firstly, observations lager than a threshold are treated as unrealistic and are not assimilated. Secondly, observations leading to innovations (observations minus the model-simulated values) higher than a maximum deviation are omitted. For $PM_{2.5}$, $PM_{10}$, $SO_2$, $NO_2$, $O_3$, and CO, the threshold in the first step is 500 μg $m^{-3}$, 700 μg

https://doi.org/10.5194/acp-2019-969
Preprint. Discussion started: 23 January 2020


Atmospheric Chemistry and Physics Discussions

158 $m^{-3}$, 200 μg $m^{-3}$, 200 μg $m^{-3}$, 200 μg $m^{-3}$, and 20 mg $m^{-3}$, respectively; the maximum deviation in the
159 second step is 120 μg $m^{-3}$, 120 μg $m^{-3}$, 60 μg $m^{-3}$, 60 μg $m^{-3}$, 60 μg $m^{-3}$, and 6 mg $m^{-3}$, respectively.

160 To verify sulfate-nitrate-ammonium partitioning, a site observation of different chemical species
161 is used in Section 4. The measurements were performed over January 14–20, 2017, and carried out on
162 the roof of IUM in Beijing (green dot in Fig. 1). A detailed description for the features of the
163 observation, including the quality assurance and quality control has been given by Su et al. (2018).
164 This study mainly uses the sulfate ($SO_4^{2-}$) and nitrate ($NO_3^-$) in this dataset.

165 **2.3 WRFDA-Chem system**

166 In this study, an aerosol/chemical assimilation capability is built within the version 4.0.3 of the
167 WRFDA system with 3DVAR algorithm. The WRFDA 3DVAR produces the analysis through the
168 minimization of a scalar objective function $J(x)$ given by

169 $$J(x) = \frac{1}{2}(x - x_b)^T B^{-1}(x - x_b) + \frac{1}{2}[H(x) - y]^T R^{-1}[H(x) - y], \quad (1)$$

170 where $x_b$ denotes the background vector, y is a vector of the observations, and $B$ and $R$ represent
171 the background and observation error covariance matrices, respectively. The covariance matrices
172 determine how close the analysis is weighted toward the background and observations. $H$ is the
173 observation operator that interpolates model grid point values to observation space and converts
174 model-predicted variables to observed quantities.

175 Generally, the implementation of WRFDA-Chem 3DVAR includes several parts: WRF-Chem
176 model and surface air pollutants observation interface to WRFDA, the addition of aerosol/chemical
177 analysis variables, the surface air pollutants observation operators, the update of observation errors,

https://doi.org/10.5194/acp-2019-969
Preprint. Discussion started: 23 January 2020


Atmospheric Chemistry and Physics Discussions

and the statistics of background error covariances for chemical analysis variables. Detailed descriptions will be presented in the following parts. It's worth mentioning that the new WRFDA-Chem system is designed with a flexible aerosol assimilation capability that can switch between different aerosol schemes. Given the fact that WRF-Chem model predicts the PM concentrations in the forms of different prognostic variables depending on the chosen aerosol scheme, the aerosol/chemical prognostic variables are given in the registry file of the WRFDA-Chem, instead of specifically defined in the code. With the help of the registry mechanism of WRF model, the prognostic variables in the entire DA process can be easily adjusted by modifying the registry file. The WRFDA-Chem system has been tested with GOCART and MOSAIC aerosol scheme, while this study focuses on the MOSAIC scheme.

#### 2.3.1 Observation operators

The WRFDA-Chem is designed to assimilate six types of surface aerosol/chemical observations, including $PM_{2.5}$, $PM_{10}$, $SO_2$, $NO_2$, $O_3$, and CO. For aerosol assimilation, the aerosol species in the MOSAIC scheme are defined as black carbon (BC), organic compounds (OCs), sulfate ($SO_4^{2-}$), nitrate ($NO_3^-$), ammonium ($NH_4^+$), sodium (NA), chloride (CL), and other inorganic compounds (OIN). To represent the aerosol size distribution, MOSAIC uses a sectional approach with different bins. This study uses four size bins with aerosol diameters ranging from 0.039–0.1, 0.1–1.0, 1.0–2.5, and 2.5–10μm. The $PM_{2.5}$ total is controlled by the 24 variables in the first three bins (8 species multiplied by 3 bins), and the $PM_{10}$ total is controlled by the 32 variables in the four bins (8 species multiplied by 4 bins). In result, the model-simulated $PM_{2.5}$ are computed by summing the 24 variables as

$$y^f_{PM_{2.5}} = \rho_d \sum_{i=1}^{3} [BC_i + OC_i + SO_{4_i} + NO_{3_i} + NH_{4_i} + CL_i + NA_i + OIN_i]. \quad (2)$$

https://doi.org/10.5194/acp-2019-969
Preprint. Discussion started: 23 January 2020


Atmospheric Chemistry and Physics Discussions

199 The model-simulated $PM_{10}$ observations are computed by summing the 32 variables as

200 $$y^f_{PM_{10}} = \rho_d \sum_{i=1}^{4}[BC_i + OC_i + SO_{4_i} + NO_{3_i} + NH_{4_i} + CL_i + NA_i + OIN_i]. \quad (3)$$

201 Correspondingly,

202 $$y^f_{PM_{10-2.5}} = \rho_d \sum_{i=4}^{4}[BC_i + OC_i + SO_{4_i} + NO_{3_i} + NH_{4_i} + CL_i + NA_i + OIN_i], \quad (4)$$

203 where $\rho_d$ is the dry-air density, which is used to convert the unit of the analysis variable (μg/kg) to
204 the observations (μg/m$^3$); $i$ denotes the bin number in the MOSAIC aerosol scheme. In the
205 experiment assimilating $PM_{2.5}$ alone, the $PM_{2.5}$ observations are used to analyze the species in first
206 three bins (Eq. 2). In the experiment assimilating $PM_{2.5}$ and $PM_{10}$ simultaneously, the $PM_{2.5}$
207 observations are used to analyze the species in first three bins (Eq. 2), and the $PM_{10\text{-}2.5}$ (PMcoarse,
208 hereafter) in the observations is used to analyze the species in the 4th bin (Eq. 4). A similar approach
209 has been adopted by Peng et al. (2018).

210 In the assimilation of the gas-phase pollutants, the model-simulated values are computed by

211 $$y^f_x = \rho_d \cdot \frac{M_x}{M_{dair}} \cdot R_x \cdot 10^3, \quad (5)$$

212 where $x$ denotes the four gas-phases pollutants as in $SO_2$, $NO_2$, $O_3$, and CO, $\rho_d$ is the dry-air density,
213 $M_x$ is the relative molecular mass for the four gas-phases pollutants, $M_{dair}$ is the relative molecular
214 mass for dry-air, and $R_x$ is the mixing ratio for the four gas-phases pollutants. Since the gas-phase
215 pollutants observations are mass concentrations in μg/m$^3$ and the analysis variables are mixing ratios
216 in ppmv, the Eq. 5 is used for the unit conversion.

https://doi.org/10.5194/acp-2019-969
Preprint. Discussion started: 23 January 2020


Atmospheric Chemistry and Physics Discussions

#### 2.3.2 Observation errors

Following Chen et al. (2019) and Peng et al. (2018), the observation error covariance matrix R in Eq. (1) is estimated from measurement error $\varepsilon_0$ and the representativeness error $\varepsilon_r$ in this study. The measurement error $\varepsilon_0$ is defined as $\varepsilon_0 = 1.0 + 0.0075 \cdot M_i$, where $M_i$ denotes the observation of the six major pollutants in unit μg/m$^3$; the representativeness error $\varepsilon_r$ is defined as $\varepsilon_r = \gamma\varepsilon_0\sqrt{\frac{\Delta x}{L}}$. where $\gamma$ is an adjustable parameter scaling (set as 0.5), $\Delta$x is the grid spacing (40.5 km in our case) and L is the radius of influence of the observation (set to 2 km). These parameter settings are based on the sensitivity tests by Chen et al. (2019). The total observation error ($\varepsilon_x$) is computed as $\varepsilon_x = \sqrt{\varepsilon_{0_x}^2 + \varepsilon_{r_x}^2}$, where $x$ denotes the six major pollutants as in $PM_{2.5}$, $PM_{10}$, $SO_2$, $NO_2$, $O_3$, and CO.

#### 2.3.3 Background error covariance

To implement the aerosol/chemical DA with the MOSAIC-4Bin scheme, this study expands the GEN_BE v2.0 (Descombes et al. 2015) to compute the **B** matrix in Eq. (1) for the 32 chemical variables as in Eq. 3 (BC, OC, $SO_4^{2-}$, $NO_3^-$, $NH_4^+$, NA, CL, and OIN in four bins), as well as the four gas-phase variables as in Eq. 5 ($SO_2$, $NO_2$, $O_3$, and CO). Cross-correlations between different aerosol/chemical variables were not considered. With the updated GEN_BE v2.0, the statistics for background error covariance, such as standard deviation, vertical and horizontal length scales, and vertical correlations, are computed for each of the aerosol/chemical variable. In this study, the background error covariance is estimated using the National Meteorological Center (NMC) method (Parrish and Derber, 1992) from one-month WRF-Chem forecasts over January 2017.

https://doi.org/10.5194/acp-2019-969
Preprint. Discussion started: 23 January 2020


Atmospheric Chemistry and Physics Discussions

236 **2.3.4 Experimental design**

237 To seek for the best forecast performance, six experiments were conducted for January 2017 in
238 this study, including NODA, PM1, PM2, ALL, ALL_3h, and ALL_1h (detailed in Table 2). NODA is
239 the control experiment without any data assimilation. The design of PM1, PM2, and ALL is to
240 investigate the assimilation impacts of $PM_{2.5}$, PMcoarse, and gas-phase pollutants ($SO_2$, $NO_2$, $O_3$, CO)
241 step-by-step.

242 The NODA experiment initialized a new WRF-Chem forecast every 6-h between 00:00 UTC, 20
243 December 2016 and 18:00 UTC 31 January 2017, in which the aerosol/chemical fields were simply
244 carried over from cycle to cycle, and the meteorological initial condition/boundary conditions were
245 updated from GFS data every 6-h. The first 10 days were treated as the spin up period, and only
246 simulations in January were used in the following analyses. The PM1, PM2, and ALL experiments
247 updated the chemical IC using the WRFDA-Chem system every 6-h starting from 00:00 UTC, 1
248 January. The background of the first cycle was obtained from the NODA experiment, and all
249 subsequent cycles were derived from the 6-h forecast of the previous cycle. The only difference
250 between PM1, PM2, and ALL experiments is that PM1 only assimilated $PM_{2.5}$ observations; PM2
251 assimilated $PM_{2.5}$ and PMcoarse ($PM_{10-2.5}$) simultaneously; ALL assimilated $PM_{2.5}$, $PM_{10-2.5}$, $SO_2$, $NO_2$,
252 $O_3$, and CO together.

253 In view of the cycling frequency is an important aspect in the DA strategy, especially for 3DVAR,
254 two more experiments assimilating all the six major pollutants with different cycling frequencies are
255 further conducted, in which the ALL_3h and ALL_1h experiments assimilate the data with 3-h and 1-

https://doi.org/10.5194/acp-2019-969
Preprint. Discussion started: 23 January 2020


Atmospheric Chemistry and Physics Discussions

256 h cycling frequency, respectively. To investigate the forecast improvements, a 24-h forecast is
257 initialized for all the experiments at 00:00 UTC of each day.

258 **3. Performance of the WRFDA-Chem system**

259 **3.1 Impact on analyses**

260 To evaluate the performance of the WRFDA-Chem system, the impact on analyses is firstly
261 investigated. Figure 2 presents the domain-averaged bias and root-mean-square-error (RMSE) of the
262 analysis at 00 UTC over January 1-31, 2017. For $PM_{2.5}$ (Fig. 2a), the NODA experiment displays a
263 general overestimation of 36.60 μg/m$^3$, along with a large RMSE of 70.41 μg/m$^3$. After DA, in the
264 PM1, PM2, and ALL experiments, the bias of $PM_{2.5}$ drops to 5.62 μg/m$^3$
265 , 5.19 μg/m$^3$, and 5.98 μg/m$^3$, respectively; the RMSE drops to 22.10 μg/m$^3$, 22.84 μg/m$^3$, and 23.15
266 μg/m$^3$, respectively.

267 In the analyses of $PM_{10}$, it is noted that the PM1 experiment has a larger bias than the NODA run
268 (Fig. 2b). To explain this phenomenon, Figure 3 presents the monthly mean difference between $PM_{10}$
269 and $PM_{2.5}$ ($PM_{10}$ minus $PM_{2.5}$, PMcoarse) in the analysis. In the observation, the PMcoarse generally
270 increases from south to north, reaching above 50 μg/m$^3$ over northern China (Fig. 3a). However, the
271 PMcoarse in the NODA experiment (with an average of 5.47 μg/m$^3$) is much smaller than that in the
272 observation (with an average of 39.13 μg/m$^3$). This result suggests that the WRF-Chem model failed
273 to reasonably represent the PMcoarse, which is actually the 4$^{th}$ bin of the aerosol species in the
274 MOSAIC scheme. Under this circumstance, when the assimilation of $PM_{2.5}$ trying to reduce its evident
275 overestimation (Fig. 2a), components in the first three bins (within 2.5 μm) of $PM_{10}$ decrease
276 dramatically. Meanwhile, since the simulated PMcoarse is too small, the $PM_{10}$ variates are eventually

https://doi.org/10.5194/acp-2019-969
Preprint. Discussion started: 23 January 2020


Atmospheric Chemistry and Physics Discussions

277 dominated by the adjustment of $PM_{2.5}$. In result, the assimilation of $PM_{2.5}$ causes a large negative bias
278 in the $PM_{10}$ analysis (Fig. 2b). Correspondingly, compared to the NODA run, the PMcoarse in the PM1
279 experiment exhibit no significant changes (only slightly decrease) in the analysis (Figs. 3b and 3c) and
280 also in the forecast (Fig 3f).

281 To overcome this issue, several adjustments have been adapted in the $PM_{10}$ assimilation: instead
282 of using the $PM_{10}$ observations directly, the PMcoarse is used to analyze the species in the 4$^{th}$ bin (Eq.
283 4); to reflect the large uncertainty of the simulated PMcoarse and to appropriately weighting the model
284 and observation errors, the background error covariance of the PMcoarse (species in the 4$^{th}$ bin) is
285 arbitrarily inflated (inflation factor 1 is normally used and 90 is selected after tuning). By this means,
286 after assimilating the $PM_{10}$ observations, the PM2 and ALL experiments exhibit similar distributions
287 in the PMcoarse (Figs. 3d-e, with an average of 34.58 $\mu g/m^3$ and 34.68 $\mu g/m^3$) as in the observation
288 (with an average of 39.13 $\mu g/m^3$). Correspondingly, compared to the NODA experiment, evident
289 improvements for $PM_{10}$ analysis appear in the PM2 and ALL experiments, in which the bias and RMSE
290 drops evidently (Fig. 2b). Overall, the DA experiments exhibit strong contributions to the analyses of
291 $PM_{2.5}$ and $PM_{10}$, suggesting that the WRFDA-Chem system works effectively in updating the initial
292 conditions.

293 As for the analyses of gaseous pollutants (Figs. 2c-2f), large improvements can be seen in the ALL
294 experiment by further assimilating $SO_2$, $NO_2$, $O_3$, and CO. Compared to the PM2 experiment, although
295 the bias and RMSE for $PM_{2.5}$ and $PM_{10}$ in the ALL experiment is slightly larger, the bias for the four
296 gaseous pollutants decrease from 4.74 $\mu g/m^3$, -4.59 $\mu g/m^3$, 4.92 $\mu g/m^3$, and -8.31 $mg/m^3$ (PM2
297 experiment) to -1.68 $\mu g/m^3$, -1.25 $\mu g/m^3$, -0.31 $\mu g/m^3$, and -0.18 $mg/m^3$ (ALL experiment),
298 respectively, and the corresponding RMSE drops from 37.87 $\mu g/m^3$, 15.39 $\mu g/m^3$, 21.04 $\mu g/m^3$, and

https://doi.org/10.5194/acp-2019-969
Preprint. Discussion started: 23 January 2020


Atmospheric Chemistry and Physics Discussions

299 1.11 mg/m$^3$ (PM2 experiment) to 23.85 μg/m$^3$, 9.70 μg/m$^3$, 8.62 μg/m$^3$, and 0.43 mg/m$^3$ (ALL
300 experiment). In general, by assimilating all the six major pollutants, the ALL experiment displays the
301 largest improvement in the analyses of gaseous pollutants among all the experiments, along with a
302 comparable improvement in the analyses of the aerosols.

303 Due to lack of vertical information within the observations, the common mathematical solution to
304 use the surface total mass observations to analyze multiple 3-D fields variables is to utilize prior
305 information in the background. As show in Fig. 4, based on vertical correlations specified in the
306 background error covariance, the observation impact spreads to a certain height, even though the
307 analysis variables used in the observation operator (Eq. 2-5) are only at the lowest model level. It is
308 also noted that observations contribute differently among the analysis variables. Corresponding to the
309 strong overestimation of $PM_{2.5}$ (Fig. 2a), all the three DA experiments (PM1, PM2 and ALL) tend to
310 reduce the $PM_{2.5}$ below 6 km; corresponding to the distinct underestimation for CO (Fig. 2f), the
311 experiment assimilating CO (ALL experiment) increases the value below 9 km. Relative small analysis
312 increments are shown in the other three gas pollutants ($SO_2$, $NO_2$, and $O_3$).

313 **3.2 Forecast improvements**

314 After illustrating the effect of WRFDA-Chem on the analyses, this section further investigates the
315 forecast performances based on the new analyses. A 24-h forecast is performed at each 00 UTC from
316 1 to 31 January 2017. The forecast error statistics, including bias, RMSE and correlation, are computed
317 by verifying against the surface observations at 531 stations over China.

318 As shown in Fig. 5, model performs relatively poor in the forecast of aerosols without DA. For
319 $PM_{2.5}$, the average bias, RMSE, and correlation over 0-24 h are 31.17 μg/m$^3$, 88.99 μg/m$^3$, and 0.41,

https://doi.org/10.5194/acp-2019-969
Preprint. Discussion started: 23 January 2020


Atmospheric Chemistry and Physics Discussions

320 respectively (Tab. 3). As expected, all the DA experiments improve the forecasts evidently. Along
321 with the forecast range, distinct improvements on bias, RMSE and correlation last from 0 to 24 h.
322 Averaging over 0-24 h, the improvement percentage for bias, RMSE and correlation reach up to 72.4%,
323 39.0%, and 43.9%, respectively. It is also noted that $PM_{2.5}$ observation is the dominant data source in
324 improving $PM_{2.5}$ forecast. As for $PM_{10}$, distinct improvements on RMSE and correlation can be seen
325 from 0 to 24 h. Especially after assimilating the PMcoarse ($PM_{10-2.5}$ in PM2 and All experiments), the
326 averaged improvement percentage for RMSE and correlation reach up to about 26.2 % and 55.5%. For
327 bias, since the statistics are averaged over the 531 stations, the offset of large positive and negative
328 bias at different stations lead to the small averaged bias in the NODA run (see the spatial distribution
329 of bias at individual site in Section 1 of the supplementary material). Considering the DA experiments
330 exhibit distinct improvements on RMSE and correlation, WRFDA-Chem still provides a general
331 positive contribution to the $PM_{10}$ forecast.

332 Figure 6 presents the averaged forecast error statistics for $SO_2$, $NO_2$, $O_3$, and CO with respect to
333 forecast range. In PM1 and PM2 experiments that do not assimilate the gas-phase observations, no
334 significant changes appear in the forecasts of the gaseous pollutants compared to the NODA run; after
335 assimilating the gas-phase observations, the ALL experiment shows evident improvements in all the
336 four gaseous pollutants, in which the improvements for $SO_2$, $NO_2$, and $O_3$ are more significant in 0-10
337 h, and the improvements for CO last up to 24 h. According to the numbers shown in Table 3, for $SO_2$,
338 $NO_2$, $O_3$, and CO, the average bias (RMSE) in the ALL experiment decreases by 13.4%, 42.3%, 74.0%,
339 and 74.5% (13.4%, 5.3%, 11.3%, and 33.7%), compared to the NODA run, and the average correlation
340 increases by 34.8%, 9.6%, 40.0%, and 103.5%, respectively. It is worth noting that the WRFDA-Chem
341 system has a positive impact on the forecast of $NO_2$ and $O_3$ by merely analyzing the IC. Since $NO_2$

https://doi.org/10.5194/acp-2019-969
Preprint. Discussion started: 23 January 2020


Atmospheric Chemistry and Physics Discussions

and $O_3$ are related to complex photochemical reaction processes, the assimilation of $NO_2$ and $O_3$ usually does not work well as other gas-phase pollutants on the forecast aspect, even with both emission and IC analyzed (Peng et al. 2018). In result, the aerosol/chemical assimilation based on WRFDA-Chem could not only contribute to the conventional aerosol forecasts in operational applications, but also provide valuable help in the emerging study demands for gaseous pollutants, especially $O_3$.

Air Quality Index (AQI), which is used for reporting daily air quality and issuing alarms, is one of the service products of RMAPS-Chem operational air quality model over Northern China. Generally, AQI is classified into six levels rating from good to hazardous: 0-50 (level 1), 51-100 (level 2), 101-150 (level 3), 151-200 (level 4), 201-300 (level 5), and 300+ (Level 6). Similar to previous studies (Kumar and Goyal 2011; Tao et al. 2015; Zheng et al. 2014), AQI is calculated for the six major pollutants. The pollutant with the highest AQI level is deemed as the "main pollutant" and its AQI determines the overall AQI level. Accordingly, the accurate forecast of AQI requires the overall good performances of the six pollutants. To reflect the integrated DA effect of aerosols and gas-phase pollutants, the threat score (TS, calculation methodology in Section 2 of the supplemental material) for AQI at each AQI level is further analyzed. As shown in Fig. 7, in the beginning of the forecast, DA experiments (PM1, PM2 and ALL) increase the TS remarkably at all AQI levels, and then gradually decrease (quickly drop) with the forecast range at AQI levels 2-6 (AQI level 1). Nevertheless, for the polluted situations with AQI levels 3-6, evident improvements can be seen from 0 to 24h in all the DA experiments, in which the average TS increase from 0.19, 0.09, 0.16, and 0.19 (NODA experiment) to about 0.27, 0.16, 0.27, and 0.26 (DA experiments), respectively. For heavy polluted situations with AQI levels 5-6 (Figs. 7e-f), compared to the PM1 case, TS experiences a further increase in the PM2

https://doi.org/10.5194/acp-2019-969
Preprint. Discussion started: 23 January 2020


Atmospheric Chemistry and Physics Discussions

and ALL experiments after assimilating the PMcoarse ($PM_{10-2.5}$). This result indicates that for heavy polluted events during this period (January 2017), $PM_{2.5}$ and $PM_{10}$ could be the "main pollutant" that contributes the most to the AQI.

In general, the new WRFDA-Chem evidently improves the aerosol/chemical forecasting. Based on the assimilation of the six major pollutants, the chemical ICs are improved distinctly and a better forecast performance is acquired up to 24 hours. Among different experiments, the ALL experiment displays the best forecast error statistics for most of the major pollutants along with the highest TS for AQI. In the following operational applications, it is recommended to assimilate the six major pollutants simultaneously, which will help to get better analyses and forecast skills on the whole.

### 3.3 Response to DA cycling frequency

Cycling frequency is an important aspect in the DA strategy. However, the responses toward IC updating could be different among the pollutants. To figure out this issue and to provide helpful references for future applications, DA experiments with different cycling frequencies were analyzed in this section.

Figure 8 shows the domain-averaged bias and RMSE of the analysis as in Fig. 2, but for experiments with different DA frequencies (ALL_6h, ALL_3h and ALL_1h). Except for $O_3$, most of the variables display a gradual improvement with the increase of cycling frequency. For example, from NODA run to the 6-h cycling experiment, and then to the 3-h and 1-h cycling experiment, the bias (RMSE) for $PM_{2.5}$ gradually decrease from 36.60 $\mu g/m^3$ (70.41 $\mu g/m^3$) to 5.98 $\mu g/m^3$ (23.15 $\mu g/m^3$), and then to 5.41 $\mu g/m^3$ (21.32 $\mu g/m^3$) and 4.30 $\mu g/m^3$ (18.54 $\mu g/m^3$). Similar results also exist in the bias for $SO_2$, $NO_2$, and CO, as well as the RMSE for $PM_{10}$, $SO_2$, and CO. In accordance with the

https://doi.org/10.5194/acp-2019-969
Preprint. Discussion started: 23 January 2020


Atmospheric Chemistry and Physics Discussions

385 gradual improvements in the analyses, the forecast skills increase with the cycling frequency in most
386 of the variables except $O_3$ (Figs. 9-10). Especially for the forecasts of aerosols, evident gradual
387 improvements can be seen from 0 to 24 h. From the 6-h cycling experiment to the 3-h and the 1-h
388 cycling experiment, the averaged decrease percentage of RMSE for $PM_{2.5}$ ($PM_{10}$) enlarges from 38.76%
389 to 41.27% and 44.21% (27.31% to 30.17% and 32.97%); the averaged increase percentage of
390 correlation for $PM_{2.5}$ ($PM_{10}$) enlarges from 42.82% to 49.51% and 55.58% (57.71% to 66.39% and
391 74.89%). To further investigate the integrated DA effect of aerosols and gas phase pollutants under
392 different cycling frequency, the TS for AQI is shown in Fig. 11. The forecast of air quality is improved
393 step by step with the increase of cycling frequency. On AQI levels 2-6, the TS for the ALL_1h
394 experiment situates above the ALL_3h experiment at most of the time, and followed by the ALL_6h
395 experiment. These results indicate that the frequent IC updating is helpful to further improve the
396 forecast for most of the pollutants.

397 However, the analysis and forecast of $O_3$ becomes worse under higher cycling frequencies (Fig.
398 8e and 10c). As a short-lived chemical reactive species, $O_3$ takes part in highly complex and rapid
399 photochemical reactions in association with $NO_2$ and VOC (Peng et al. 2018, Lu et al., 2019). From
400 this perspective, the performances of $O_3$ could mostly rely on the rapid photochemistry, in addition to
401 the IC. In the DA experiments, the assimilation of $NO_2$ changes the $NO_2$ concentration and leave the
402 VOC unadjusted due to the absence of VOC measurements. In result, the $NO_2$/VOC ratio which
403 determine the photochemical reactions and even regime might be changed ($O_3$ production/loss
404 direction might change). Since the relevant $NO_x$-VOC-$O_3$ reactions take place so quickly, changing
405 the $O_3$ concentration in minutes, the advantage of IC DA is competing with the disadvantage of the
406 disordered photochemistry (inaccurate $NO_2$/VOC ratios) from the unadjusted VOC and the updated $O_3$

https://doi.org/10.5194/acp-2019-969
Preprint. Discussion started: 23 January 2020


Atmospheric Chemistry and Physics Discussions

and $NO_2$, and thus the improvement of IC DA could be consumed quickly. Under this circumstance, the more frequent the $O_3$ and $NO_2$ were assimilated, the more incompatibilities could be brought into the related photochemical reactions, resulting the model performs worse in the forecast of $O_3$ under higher cycling frequencies.

According to the results above, it is better to assimilate $PM_{2.5}$, $PM_{10}$, $SO_2$ and CO every 1 h and assimilate $O_3$ and $NO_2$ every 6 h in the future applications, given the fact that the 6-h cycling experiment performs the best in the $O_3$ forecasting (Fig. 10c) and displays no significant differences in the $NO_2$ forecasting with experiments under higher cycling frequencies (Fig. 10b). It could also be helpful to assimilate the VOC along with $O_3$ and $NO_2$ after there are corresponding observations.

## 4. Indications on further model development

A higher forecast skill relies on not only better working of DA, but also better performance of the forecast model. To further improve the forecast skill, a crucial task is to understand the deficiencies in the model, while the challenge in chemistry model diagnostic is that uncertainties are from various aspects and are mixed-up in the model simulations, and the situation becomes even more complex when the reaction path is not yet revealed by laboratory. However, with the help of DA, as one aspect (IC) in the model is corrected by using observation as constraints, the deficiencies from other aspects (e.g. chemical reactions) could be more evident, and thus there could be a better chance to diagnose the deficiencies in the model. Specifically, Sulfate-nitrate-ammonium (SNA) are the predominant inorganic aerosol species that contribute up to 50% of total $PM_{2.5}$ in heavy polluted events in northern China (Wang et al. 2014). In addition to the normal pathways in the MOSAIC scheme, we added $SO_2$-$NO_2$-$NO_3$ related heterogeneous reactions for high relative humidity case in WRF-Chem (Chen et al.

https://doi.org/10.5194/acp-2019-969
Preprint. Discussion started: 23 January 2020


Atmospheric Chemistry and Physics Discussions

2016), which greatly improved the underestimated SNA simulations. Since the newly added reactions are calculated on both the concentration of precursors ($SO_2$, $NO_2$-$NO_3$) and the uptake coefficients in the model, after DA corrected the concentrations of the precursors (one aspect), the impacts of the uptake coefficients could be more evident (the other aspect than the one corrected). Ideally, if the newly added reactions depict the heterogeneous reaction processes properly, a forecast improvement on the aerosols could be expected by assimilating their gaseous precursors. Based on this notion, this section verifies the forecast of two specific aerosol species, sulfate ($SO_4^{2-}$) and nitrate ($NO_3^-$), against a size-resolved particle observation over Beijing IUM station (in view of the assimilated $SO_2$ and $NO_2$ are the corresponding gaseous precursors of these aerosol species), aiming to explore the deficiencies in the uptake coefficients in the newly added heterogeneous reactions, and to provide beneficial indications for future model development.

Figure 12 presents the time series of sulfate and nitrate over Beijing IUM station. In the ALL experiment, after assimilating both the PM concentrations and the gaseous precursors ($SO_2$, $NO_2$), the forecasts of sulfate and nitrate become even worse than the PM2 experiment which only assimilates the PM concentrations. In the ALL experiment, sulfate experiences a decrease, accompanied by the average RMSE grows from 4.32 to 4.88 μg/m$^3$; nitrate exhibits an increase, accompanied by the average RMSE grows from 8.74 to 10.12 μg/m$^3$. However, compared to the PM2 experiment, the precursors ($SO_2$ and $NO_2$) are indeed improved. Figure 13 displays the analysis statistics of $SO_2$ and $NO_2$ in the ALL experiment around Beijing area (red dots in Fig. 1) on January 16, the period with the largest changes of sulfate and nitrate (Fig. 12). To correct the overestimated $SO_2$ (underestimated $NO_2$) in the background, the DA in reduces (enhances) the model value in the ALL experiment, making it closer to the observations.

https://doi.org/10.5194/acp-2019-969
Preprint. Discussion started: 23 January 2020


Atmospheric Chemistry and Physics Discussions

450 It should be mentioned that the heterogeneous reactions are added by using the sulfate-nitrate-
451 ammonium observations as constraints to tune the "observation-best-matched" uptake coefficients
452 under the scenario without DA, in which the precursor concentrations are from pure model thus not
453 very accurate. To best match the observation, when gaseous precursors are overestimated
454 (underestimated) in the model, the uptake coefficient is tuned to low-biased (high-biased) value. In
455 result, such a coefficient may no longer be suited for the cases with DA. For instance, after DA
456 reducing the overestimated $SO_2$, the uptake coefficient is still relatively low and thus the reaction from
457 $SO_2$ to sulfate will stay at a low rate (with both low value of $SO_2$ and low reaction coefficient). A
458 similar result also exists for the reaction from $NO_2$ to nitrate. From this perspective, the negative effects
459 on sulfate and nitrate in the ALL experiment may not be hard to understand (Fig. 12). Therefore, in
460 the future chemistry development, it is necessary to develop more appropriate coefficients for different
461 gaseous precursor scenarios, in which more constraints, such as precursor and species concentrations,
462 should be provided with the help of DA technique. Accordingly, further improvements on aerosol
463 forecast could be expected by assimilating their gaseous precursors.

464 According to the results above, the DA technique provides an opportunity to identify and diagnose
465 the deficiencies in the model. By correcting the precursor concentrations through DA (one aspect), the
466 deficiency of the uptake coefficients for the SNA heterogeneous reactions (the other aspect than the
467 one corrected) is revealed. In the future, besides being used to improve the forecast skill through
468 updating the IC, DA could be used as another approach to reveal the necessary developments in the
469 model.

https://doi.org/10.5194/acp-2019-969
Preprint. Discussion started: 23 January 2020


Atmospheric Chemistry and Physics Discussions

## 5. Conclusions and discussions

To improve the operational air quality forecasting over China, a flexible aerosol and gas phase pollutants assimilation capability that can switch between different aerosol schemes is developed based on the WRFDA system with 3DVAR algorithm. This flexibility is designed to address the complexity of current aerosol schemes and to facilitate future chemistry developments. In this first application, the assimilation capability of surface observations of six major pollutants, including $PM_{2.5}$, $PM_{10}$, $SO_2$, $NO_2$, $O_3$, and CO, is built with MOSAIC aerosol scheme.

Before application in the operational air quality model, capability of the WRFDA-Chem system is verified in terms of analysis and forecast performances. Using the updated system, five DA experiments (assimilate different combinations of pollutants in various frequencies) were conducted for January 2017, along with a control experiment without DA. Results exhibit that the WRFDA-Chem system evidently improves the forecast of aerosols and gas phase pollutants. On the aspect of analysis, the assimilation of different atmospheric-composition observation reduces the bias and RMSE in the IC remarkably (e.g. by about 38%, 26%, and 10-30% in the RMSE for $PM_{2.5}$, $PM_{10}$, and gas phase pollutants); on the aspect of forecast skill, better performances are acquired up to 24 hours with about 10-40% (30-50%) improvements in the RMSE (correlation) for different pollutants. Among different experiments, the one assimilating all the six pollutants displays the best forecast error statistics for most of the pollutants along with the highest TS for AQI. In future applications, to get a better analysis and forecast skill in general, it is recommended to assimilate the six major pollutants simultaneously.

As the cycling frequency is an important aspect in the DA strategy, DA experiments with various cycling frequencies are also analyzed. Results exhibit that the responses toward IC updating are

https://doi.org/10.5194/acp-2019-969
Preprint. Discussion started: 23 January 2020


Atmospheric Chemistry and Physics Discussions

different among the pollutants. For $PM_{2.5}$, $PM_{10}$, $SO_2$, and CO, the forecast skills increase with the DA frequency; for $O_3$, although improvements are acquired at the 6-h cycling frequency, the advantage of more frequent IC DA could be consumed by the disordered photochemistry (inaccurate $NO_2$/VOC ratios) due to the unadjusted VOC and the updated $O_3$ and $NO_2$ from DA. In future applications, it is better to assimilate $PM_{2.5}$, $PM_{10}$, $SO_2$, and CO every 1 h and assimilate $O_3$ and $NO_2$ every 6 h. It might also be helpful to assimilate VOC simultaneously with $O_3$ and $NO_2$ after there are corresponding measurements.

By investigating the effect of assimilating gaseous precursors on the forecast of related aerosols, the deficiencies in the WRF-Chem model are further revealed. The uptake coefficients for Sulfate-Nitrate-Ammonium heterogeneous reactions in the model are found out to be not appropriate in the applications with gaseous precursors ($SO_2$ and $NO_2$) assimilations, since they were originally tuned under the gaseous precursor scenarios without DA and the biases from the two aspects (SNA reactions and IC DA) were just compensated. In the future chemistry development, it is necessary to develop appropriate coefficients for different gaseous precursor scenarios, in which more constraints, such as precursor and species concentrations, should be provided with the help of DA technique.

Contributed by the flexible aerosol assimilation capability of the WRFDA-Chem system, development for other aerosol schemes targeting different regions in Asia is undergoing. In the next step, study will focus on assimilating chemical observations from different observing platforms, such as satellite AOD observations, which contains more information over the areas with sparse surface observations. In addition, more advanced DA techniques, such as 4DVAR and Hybrid DA, could be taken into consideration in further developing the aerosol/chemical DA system.

https://doi.org/10.5194/acp-2019-969
Preprint. Discussion started: 23 January 2020


Atmospheric Chemistry and Physics Discussions

## Code and data availability

The WRF-Chem code used in this study is the public release version available at https://www2.mmm.ucar.edu/wrf/users/download/get_sources.html#WRF-Chem. The WRFDA code in this study is developed based on the public release version available at https://www2.mmm.ucar.edu/wrf/users/download/get_sources.html#WRFDA, and the developed WRFDA-Chem code could be incorporated into the public release version at appropriate time. The example run directory and dataset for this paper are available upon request from the corresponding authors (liuz@ucar.edu and dchen@ium.cn) and Wei Sun (weisun0416@gmail.com).

## Author contributions

WS and ZL conducted development of DA system. ZL, DC, WS, and MC designed research, WS performed experiments and analyzed results, PZ provided PM species observations, and WS and DC wrote the paper with contributions from all co-authors.

## Acknowledgement

This work was supported by the National Key R&D Program on Monitoring, Early Warning and Prevention of Major Natural Disasters under grant (2017YFC1501406), and Basic R&D special fund for central level, scientific research institutes (IUMKYSZHJ201701, IUMKY201807) of China. NCAR is sponsored by the US National Science Foundation.

https://doi.org/10.5194/acp-2019-969
Preprint. Discussion started: 23 January 2020


Atmospheric Chemistry and Physics Discussions

## Competing interests

The authors declare that they have no conflict of interest.

## References

Bannister, R., 2017: A review of operational methods of variational and ensemble-variational data assimilation. *Quarterly Journal of the Royal Meteorological Society*, **143,** 607-633.

Chen, D., Z. Liu, J. Fast, and J. Ban, 2016: Simulations of sulfate–nitrate–ammonium (SNA) aerosols during the extreme haze events over northern China in October 2014. *Atmospheric Chemistry and Physics*, **16,** 10707-10724.

Chen, D., Z. Liu, J. Ban, P. Zhao, and M. Chen, 2019: Retrospective analysis of 2015–2017 wintertime PM 2.5 in China: response to emission regulations and the role of meteorology. *Atmospheric Chemistry and Physics*, **19,** 7409-7427.

Chen, F., and J. Dudhia, 2001: Coupling an advanced land surface–hydrology model with the Penn State–NCAR MM5 modeling system. Part I: Model implementation and sensitivity. *Monthly Weather Review*, **129,** 569-585.

Chou, M.-D., and M. J. Suarez, 1994: An efficient thermal infrared radiation parameterization for use in general circulation models.

Descombes, G., T. Auligné, F. Vandenberghe, D. Barker, and J. Barre, 2015: Generalized background error covariance matrix model (GEN_BE v2. 0). *Geoscientific Model Development*, **8,** 669-696.

https://doi.org/10.5194/acp-2019-969
Preprint. Discussion started: 23 January 2020




547 Fan, S., and Coauthors, 2016: Introduction of Rapid-refresh Multi-scale Analysis and Prediction
548 System-short time (RMAP-ST) over Northern China (in Chinese). *33th Annual Meeting of*
549 *Chinese Meteorological Society*.
550 Fast, J. D., and Coauthors, 2006: Evolution of ozone, particulates, and aerosol direct radiative forcing
551 in the vicinity of Houston using a fully coupled meteorology-chemistry-aerosol model. *Journal*
552 *of Geophysical Research: Atmospheres*, **111**.
553 Fu, Y., H. Liao, and Y. Yang, 2019: Interannual and decadal changes in tropospheric ozone in China
554 and the associated chemistry-climate interactions: A review. Advances in Atmospheric Sciences,
555 **36**, 975-993.
556 Grell, G. A., and D. Dévényi, 2002: A generalized approach to parameterizing convection combining
557 ensemble and data assimilation techniques. *Geophysical Research Letters*, **29,** 38-31-38-34.
558 Grell, G. A., S. E. Peckham, R. Schmitz, S. A. McKeen, G. Frost, W. C. Skamarock, and B. Eder,
559 2005: Fully coupled "online" chemistry within the WRF model. *Atmospheric Environment*, **39,**
560 6957-6975.
561 He, K., 2012: Multi-resolution emission Inventory for China (MEIC): model framework and 1990–
562 2010 anthropogenic emissions, presented on the international Global Atmospheric Chemistry
563 Conference, 17–21 September 2012, Beijing, China.
564 Hong, S.-Y., Y. Noh, and J. Dudhia, 2006: A new vertical diffusion package with an explicit treatment
565 of entrainment processes. *Monthly weather review*, **134,** 2318-2341.
566 Huang, X., Y. Song, C. Zhao, M. Li, T. Zhu, Q. Zhang, and X. Zhang, 2014: Pathways of sulfate
567 enhancement by natural and anthropogenic mineral aerosols in China. *Journal of Geophysical*
568 *Research: Atmospheres*, **119,** 14,165-114,179.

https://doi.org/10.5194/acp-2019-969
Preprint. Discussion started: 23 January 2020


Atmospheric Chemistry and Physics Discussions

569 Jiang, Z., Z. Liu, T. Wang, C. S. Schwartz, H. C. Lin, and F. Jiang, 2013: Probing into the impact of
570 3DVAR assimilation of surface PM10 observations over China using process analysis. *Journal*
571 *of Geophysical Research: Atmospheres*, **118,** 6738-6749.
572 Kumar, A., and P. Goyal, 2011: Forecasting of daily air quality index in Delhi. *Science of the Total*
573 *Environment*, **409,** 5517-5523.
574 Lei, Y., Q. Zhang, K. He, and D. Streets, 2011: Primary anthropogenic aerosol emission trends for
575 China, 1990–2005. *Atmospheric Chemistry and Physics*, **11,** 931-954.
576 Li, M., and Coauthors, 2014: Mapping Asian anthropogenic emissions of non-methane volatile organic
577 compounds to multiple chemical mechanisms. *Atmos. Chem. Phys*, **14,** 5617-5638.
578 Liu, Z., Q. Liu, H. C. Lin, C. S. Schwartz, Y. H. Lee, and T. Wang, 2011: Three-dimensional
579 variational assimilation of MODIS aerosol optical depth: Implementation and application to a
580 dust storm over East Asia. Journal of Geophysical Research: Atmospheres, 116 (D23).
581 Lu, X., and Coauthors, 2019: Exploring 2016–2017 surface ozone pollution over China: source
582 contributions and meteorological influences. Atmospheric Chemistry and Physics, **19**, 8339-8361.
583 McHenry, J. N., J. M. Vukovich, and N. C. Hsu, 2015: Development and implementation of a remote-
584 sensing and in situ data-assimilating version of CMAQ for operational PM2. 5 forecasting. Part
585 1: MODIS aerosol optical depth (AOD) data-assimilation design and testing. *Journal of the Air*
586 *& Waste Management Association*, **65,** 1395-1412.
587 McKeen, S., and Coauthors, 2009: An evaluation of real-time air quality forecasts and their urban
588 emissions over eastern Texas during the summer of 2006 Second Texas Air Quality Study field
589 study. *Journal of Geophysical Research: Atmospheres*, **114**.

https://doi.org/10.5194/acp-2019-969
Preprint. Discussion started: 23 January 2020




590 Mlawer, E. J., S. J. Taubman, P. D. Brown, M. J. Iacono, and S. A. Clough, 1997: Radiative transfer
591 for inhomogeneous atmospheres: RRTM, a validated correlated-k model for the longwave.
592 *Journal of Geophysical Research: Atmospheres*, **102,** 16663-16682.
593 Nie, W., and Coauthors, 2014: Polluted dust promotes new particle formation and growth. *Scientific*
594 *reports*, **4,** 6634.
595 Pang, J., Z. Liu, X. Wang, J. Bresch, J. Ban, D. Chen, and J. Kim, 2018: Assimilating AOD retrievals
596 from GOCI and VIIRS to forecast surface PM2. 5 episodes over Eastern China. *Atmospheric*
597 *environment*, **179,** 288-304.
598 Peng, Z., Z. Liu, D. Chen, and J. Ban, 2017: Improving PM 2. 5 forecast over China by the joint
599 adjustment of initial conditions and source emissions with an ensemble Kalman filter.
600 *Atmospheric Chemistry and Physics*, **17,** 4837-4855.
601 Peng, Z., and Coauthors, 2018: The impact of multi-species surface chemical observation assimilation
602 on air quality forecasts in China. *Atmospheric Chemistry and Physics*, **18,** 17387-17404.
603 Sandu, A., and T. Chai, 2011: Chemical data assimilation—An overview. *Atmosphere*, **2,** 426-463.
604 Schutgens, N., T. Miyoshi, T. Takemura, and T. Nakajima, 2010: Applying an ensemble Kalman filter
605 to the assimilation of AERONET observations in a global aerosol transport model. *Atmospheric*
606 *Chemistry and Physics*, **10,** 2561-2576.
607 Schwartz, C. S., Z. Liu, H. C. Lin, and S. A. McKeen, 2012: Simultaneous three-dimensional
608 variational assimilation of surface fine particulate matter and MODIS aerosol optical depth.
609 *Journal of Geophysical Research: Atmospheres*, **117**.
610 Sekiyama, T., T. Tanaka, A. Shimizu, and T. Miyoshi, 2010: Data assimilation of CALIPSO aerosol
611 observations. *Atmospheric Chemistry and Physics*, **10,** 39-49.

https://doi.org/10.5194/acp-2019-969
Preprint. Discussion started: 23 January 2020




612 Su, J., P. Zhao, and Q. Dong, 2018: Chemical compositions and liquid water content of size-resolved
613 aerosol in Beijing. *Aerosol Air Qual. Res*, **18,** 680-692.
614 Tang, X., J. Zhu, Z. Wang, and A. Gbaguidi, 2011: Improvement of ozone forecast over Beijing based
615 on ensemble Kalman filter with simultaneous adjustment of initial conditions and emissions.
616 *Atmospheric Chemistry and Physics*, **11,** 12901-12916.
617 Tang, X., and Coauthors, 2013: Inversion of CO emissions over Beijing and its surrounding areas with
618 ensemble Kalman filter. *Atmospheric environment*, **81,** 676-686.
619 Tao, J., L. Zhang, J. Gao, H. Wang, F. Chai, and S. Wang, 2015: Aerosol chemical composition and
620 light scattering during a winter season in Beijing. *Atmospheric Environment*, **110,** 36-44.
621 Wang, G., and Coauthors, 2016: Persistent sulfate formation from London Fog to Chinese haze.
622 *Proceedings of the National Academy of Sciences*, **113,** 13630-13635.
623 Wang, L., and Coauthors, 2013: The 2013 severe haze over the southern Hebei, China: model
624 evaluation, source apportionment, and policy implications. *Atmospheric Chemistry & Physics*
625 *Discussions*, **13**.
626 Wang, Y., and Coauthors, 2014: Enhanced sulfate formation during China's severe winter haze episode
627 in January 2013 missing from current models. *Journal of Geophysical Research: Atmospheres*,
628 **119,** 10,425-410,440.
629 Wild, O., X. Zhu, and M. J. Prather, 2000: Fast-J: Accurate simulation of in-and below-cloud
630 photolysis in tropospheric chemical models. *Journal of Atmospheric Chemistry*, **37,** 245-282.
631 Xie, Y., and Coauthors, 2015: Enhanced sulfate formation by nitrogen dioxide: Implications from in
632 situ observations at the SORPES station. *Journal of Geophysical Research: Atmospheres*, **120,**
633 12679-12694.

https://doi.org/10.5194/acp-2019-969
Preprint. Discussion started: 23 January 2020


Atmospheric Chemistry and Physics Discussions

634 Yu, M., S. Miao, and H. Zhang, 2018: Uncertainties in the Impact of Urbanization on Heavy Rainfall:
635 Case Study of a Rainfall Event in Beijing on 7 August 2015. *Journal of Geophysical Research:*
636 *Atmospheres*, **123,** 6005-6021.
637 Zaveri, R. A., and L. K. Peters, 1999: A new lumped structure photochemical mechanism for large-
638 scale applications. *Journal of Geophysical Research: Atmospheres*, **104,** 30387-30415.
639 Zaveri, R. A., R. C. Easter, J. D. Fast, and L. K. Peters, 2008: Model for simulating aerosol interactions
640 and chemistry (MOSAIC). *Journal of Geophysical Research: Atmospheres*, **113**.
641 Zhang, Q., and Coauthors, 2009: Asian emissions in 2006 for the NASA INTEX-B mission.
642 *Atmospheric Chemistry and Physics*, **9,** 5131-5153.
643 Zheng, B., and Coauthors, 2015: Heterogeneous chemistry: a mechanism missing in current models to
644 explain secondary inorganic aerosol formation during the January 2013 haze episode in North
645 China. *Atmospheric Chemistry and Physics (Online)*, **15**.
646 Zheng, S., C.-X. Cao, and R. P. Singh, 2014: Comparison of ground based indices (API and AQI) with
647 satellite based aerosol products. *Science of the Total Environment*, **488,** 398-412.

648 **Tables and Figures**

649 **Table 1.** WRF-Chem model configurations.

650 **Table 2.** The detail setting of six experiments and the purposes.

651 **Table 3.** Averaged bias (units: μg/m$^3$), RMSE (units: μg/m$^3$), and correlation over forecast hour 0-24
652 h for different variables and different experiments. The statistics for gas phase pollutants in PM1 and

https://doi.org/10.5194/acp-2019-969
Preprint. Discussion started: 23 January 2020




653 PM2 experiments are highly close to the results in NODA experiment, and thus leave with blank in
654 the table.

655 **Figure 1.** Computation domain. Dots depict surface observations with 531 stations spreading over
656 China. The red dots indicate the observations around Beijing.

657 **Figure 2.** Averaged bias (color bar, left y-axis) and RMSE (hallow bar, right y-axis) of the analysis at
658 00 UTC over January 1-31, 2017 for (a) $PM_{2.5}$, (b) $PM_{10}$, (c) $SO_2$, (d) $NO_2$, (e) $O_3$ and (f) CO in different
659 experiments, verified against the surface observations of 531 stations in China. The blue, red, green
660 and gray shaded bars denote the bias of the experiment NODA, PM1, PM2, ALL, respectively; the
661 corresponding hallow bars denote the RMSE of these experiments. Units of the y-axis are $\mu g/m^3$ in
662 Figs. 2a-e and $mg/m^3$ in Fig. 2f.

663 **Figure 3.** Averaged PMcoarse ($PM_{10\text{-}2.5}$, units: $\mu g/m^3$) at 00 UTC over January 1-31, 2017 in (a)
664 observation and four experiments (b) NODA, (c) PM1, (d) PM2, (e) ALL, and (f) averaged bias (units:
665 $\mu g/m^3$) for PMcoarse in different experiments as a function of forecast range (the blue, red, green and
666 gray lines denote the results of experiment NODA, PM1, PM2, ALL, respectively), verified against
667 the surface observations of 531 stations in China. The numbers on the top of each panel denote the
668 average PMcoarse concentrations over 531 stations (units: $\mu g/m^3$).

669 **Figure 4.** Vertical profile of the analysis at 00 UTC over January 1-31, 2017 for (a) $PM_{2.5}$, (b) $PM_{10}$,
670 (c) $SO_2$, (d) $NO_2$, (e) $O_3$, and (f) CO in different experiments, averaged over the 531 surface stations
671 in China. The blue, red, green and gray lines denote the results of experiment NODA, PM1, PM2, and
672 ALL, respectively. Units of the y-axis are $\mu g/m^3$ in Figs. 4a-e and $mg/m^3$ in Fig. 4f.

673 **Figure 5.** Averaged bias (units: $\mu g/m^3$), RMSE (units: $\mu g/m^3$), and correlation for (a) $PM_{2.5}$ and (b)
674 $PM_{10}$ in different experiments as a function of forecast range, verified against the surface observations

https://doi.org/10.5194/acp-2019-969
Preprint. Discussion started: 23 January 2020


Atmospheric Chemistry and Physics Discussions

675 of 531 stations in China. The blue, red, green and gray lines denote the results of experiment NODA,
676 PM1, PM2, ALL, respectively.

677 **Figure 6.** Same as Fig. 5, but for the forecast of (a) $SO_2$, (b) $NO_2$, (c) $O_3$ (units: μg/m$^3$), and (d) CO
678 (units: mg/m$^3$).

679 **Figure 7.** Averaged threat score (TS) for Air Quality Index (AQI) from AQI level 1 to level 6 (a-f) in
680 different experiments as a function of forecast range, verified against the surface observations of 531
681 stations in China. The blue, red, green and gray lines denote the results of experiment NODA, PM1,
682 PM2, and ALL, respectively. The numbers on the right of each panel denote the averaged TS from 0
683 to 24 h for different experiments.

684 **Figure 8.** Same as Fig. 2, but for the experiments of NODA, ALL_6h, ALL-3h, ALL_1h, respectively.
685 Units of the y-axis are μg/m$^3$ in Figs. 8a-e and mg/m$^3$ in Fig. 8f.

686 **Figure 9.** Averaged bias (units: μg/m$^3$), RMSE (units: μg/m$^3$), and correlation for (a) $PM_{2.5}$ and (b)
687 $PM_{10}$ in different experiments as a function of forecast range, verified against the surface observations
688 of 531 stations in China. The blue, red, green and gray lines denote the results of experiment NODA,
689 ALL_6h, ALL_3h, and ALL_1h, respectively.

690 **Figure 10.** Same as Fig. 9, but for the forecast of (a) $SO_2$, (b) $NO_2$, (c) $O_3$ (units: μg/m$^3$), and (d) CO
691 (units: mg/m$^3$).

692 **Figure 11.** Same as Fig. 7, but for the experiments of NODA, ALL_6h, ALL-3h, ALL_1h, respectively.

693 **Figure 12.** Time series of (a) sulfate, (b) nitrate over January 14-20, verified against the size-resolved
694 particle observation at IUM station. The gray, blue and red lines denote the observation and the results
695 of experiment PM2 and ALL, respectively. The numbers on the right of each panel denote the averaged
696 RMSE over January 14-20 for different experiments.

https://doi.org/10.5194/acp-2019-969
Preprint. Discussion started: 23 January 2020


Atmospheric Chemistry and Physics Discussions

697 **Figure 13.** Averaged scatter plot of (a, c) observation versus background and (b, d) observation versus

698 analysis for (a, b) $SO_2$ and (c, d) $NO_2$ around Beijing area (red dots in Fig. 1) on January 16.

699

https://doi.org/10.5194/acp-2019-969
Preprint. Discussion started: 23 January 2020


Atmospheric Chemistry and Physics Discussions

700 **Table 1.** WRF-Chem model configurations.

| | |
|---|---|
| Aerosol scheme | MOSAIC (four bins, Zaveri et al. (2008)) |
| Photolysis scheme | Fast-J (Wild et al. 2000) |
| Gas-phase chemistry | CBM-Z (Zaveri and Peters 1999) |
| Cumulus parameterization | Grell 3-D scheme |
| Short-wave radiation | Goddard Space Flight Center short-wave radiation scheme (Chou and Suarez 1994) |
| Long-wave radiation | RRTM (Mlawer et al. 1997) |
| Microphysics | Single-moment 6-class scheme (Grell and Dévényi 2002) |
| Land-surface model (LSM) | NOAH LSM (Chen and Dudhia 2001) |
| Boundary-layer scheme | YSU (Hong et al. 2006) |
| Meteorology initial and boundary conditions | GFS analysis and forecast every 6 h |
| Initial condition for chemical species | 11-day spin-up |
| Boundary conditions for chemical species | Averages of mid-latitude aircraft profiles |
| Dust and sea salt emissions | GOCART |

701

https://doi.org/10.5194/acp-2019-969
Preprint. Discussion started: 23 January 2020


Atmospheric Chemistry and Physics Discussions

**Table 2.** The detail setting of six experiments and the purposes

| Experiments | $PM_{2.5}$ assimilation | $PM_{10\text{-}2.5}$ assimilation | Gas phase ($SO_2$, $NO_2$, $O_3$, CO) assimilation | Assimilated time (UTC) | Purposes for forecast performances |
|---|---|---|---|---|---|
| NODA | No | No | No | -- | Control simulation |
| PM1 | Yes | No | No | 00, 06, 12, 18 | Basic $PM_{2.5}$ assimilation |
| PM2 | Yes | Yes | No | 00, 06, 12, 18 | $PM_{2.5}$ and $PM_{10\text{-}2.5}$ assimilation |
| ALL | Yes | Yes | Yes | 00, 06, 12, 18 | Aerosol and precursor simultaneously assimilation |
| ALL_3h | Yes | Yes | Yes | 00, 03, 06, 09, 12, 15, 18, 21 | Different assimilation frequencies on forecast performances |
| ALL_1h | Yes | Yes | Yes | 0-23, every hour | |

https://doi.org/10.5194/acp-2019-969
Preprint. Discussion started: 23 January 2020


Atmospheric Chemistry and Physics Discussions

704 **Table 3.** Averaged bias (units: μg/m$^3$), RMSE (units: μg/m$^3$), and correlation over forecast hour 0-24
705 h for different variables and different experiments. The statistics for gas phase pollutants in PM1 and
706 PM2 experiments are highly close to the results in NODA experiment, and thus leave with blank in
707 the table.

| | | NODA | PM1 | PM2 | ALL |
|---|---|---|---|---|---|
| $PM_{2.5}$ | Bias | 31.17 | 8.78 | 8.39 | 9.36 |
| | RMSE | 88.99 | 53.93 | 54.35 | 54.49 |
| | Correlation | 0.41 | 0.59 | 0.58 | 0.59 |
| $PM_{10}$ | Bias | -1.13 | -22.73 | -15.43 | -14.41 |
| | RMSE | 98.5 | 74.41 | 71.9 | 71.6 |
| | Correlation | 0.36 | 0.54 | 0.56 | 0.56 |
| $SO_2$ | Bias | 6.67 | - | - | 3.78 |
| | RMSE | 44.11 | - | - | 38.18 |
| | Correlation | 0.29 | - | - | 0.4 |
| $NO_2$ | Bias | -2.87 | - | - | -1.66 |
| | RMSE | 25.61 | - | - | 24.26 |
| | Correlation | 0.48 | - | - | 0.52 |
| $O_3$ | Bias | -3.22 | - | - | -0.84 |
| | RMSE | 31.96 | - | - | 28.36 |
| | Correlation | 0.29 | - | - | 0.41 |
| CO | Bias | -0.73 | - | - | -0.19 |
| | RMSE | 1.13 | - | - | 0.75 |
| | Correlation | 0.28 | - | - | 0.57 |

708

https://doi.org/10.5194/acp-2019-969
Preprint. Discussion started: 23 January 2020


Atmospheric Chemistry and Physics Discussions

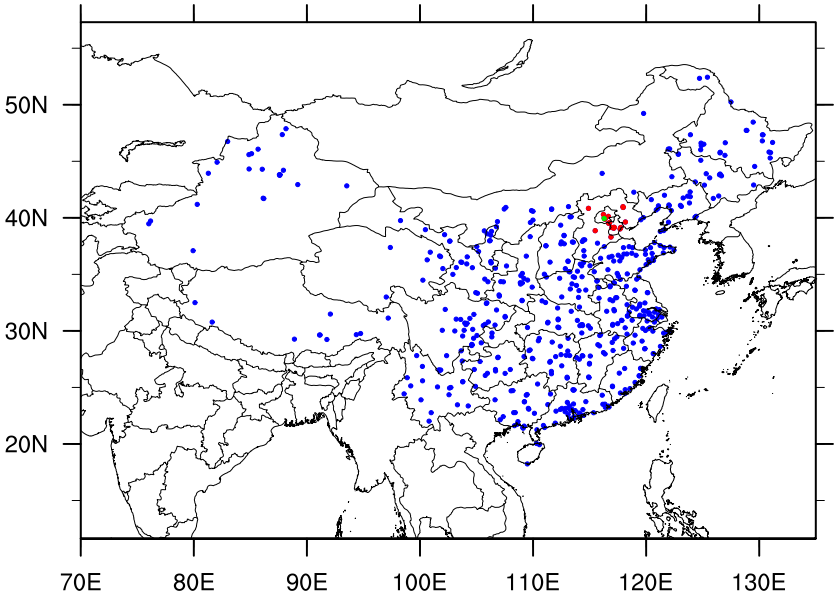


709

710 **Figure 1.** Computation domain. Dots depict surface observations with 531 stations spreading over

711 China. The red dots indicate the observations around Beijing. The green dot indicates the IUM station.

712

https://doi.org/10.5194/acp-2019-969
Preprint. Discussion started: 23 January 2020


Atmospheric Chemistry and Physics Discussions

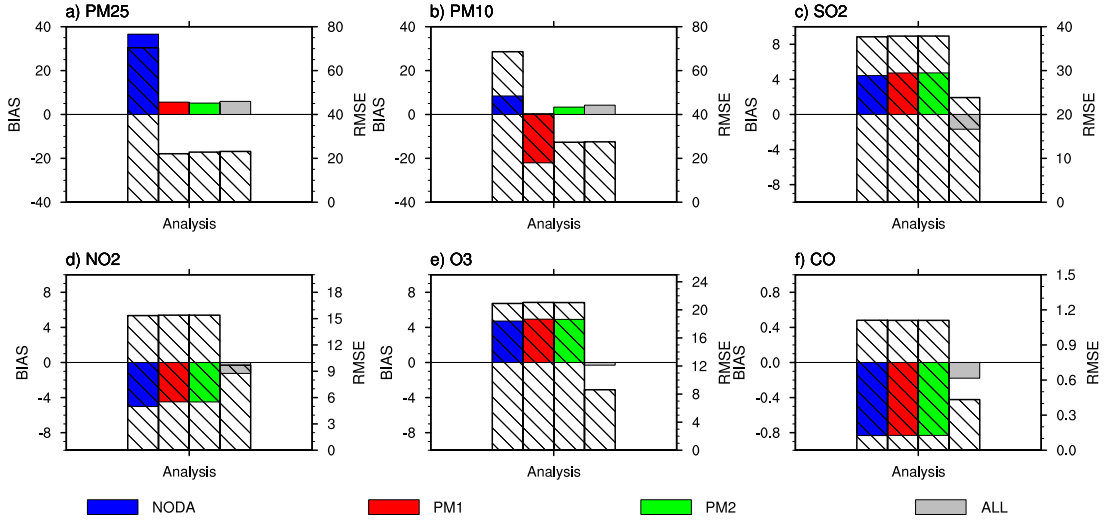


713

714 **Figure 2.** Averaged bias (color bar, left y-axis) and RMSE (hallow bar, right y-axis) of the analysis at
715 00 UTC over January 1-31, 2017 for (a) $PM_{2.5}$, (b) $PM_{10}$, (c) $SO_2$, (d) $NO_2$, (e) $O_3$ and (f) CO in different
716 experiments, verified against the surface observations of 531 stations in China. The blue, red, green
717 and gray shaded bars denote the bias of the experiment NODA, PM1, PM2, ALL, respectively; the
718 corresponding hallow bars denote the RMSE of these experiments. Units of the y-axis are $\mu g/m^3$ in
719 Figs. 2a-e and $mg/m^3$ in Fig. 2f.

720

https://doi.org/10.5194/acp-2019-969
Preprint. Discussion started: 23 January 2020


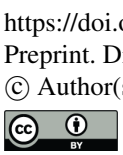

Atmospheric Chemistry and Physics Discussions
Open Access
EGU

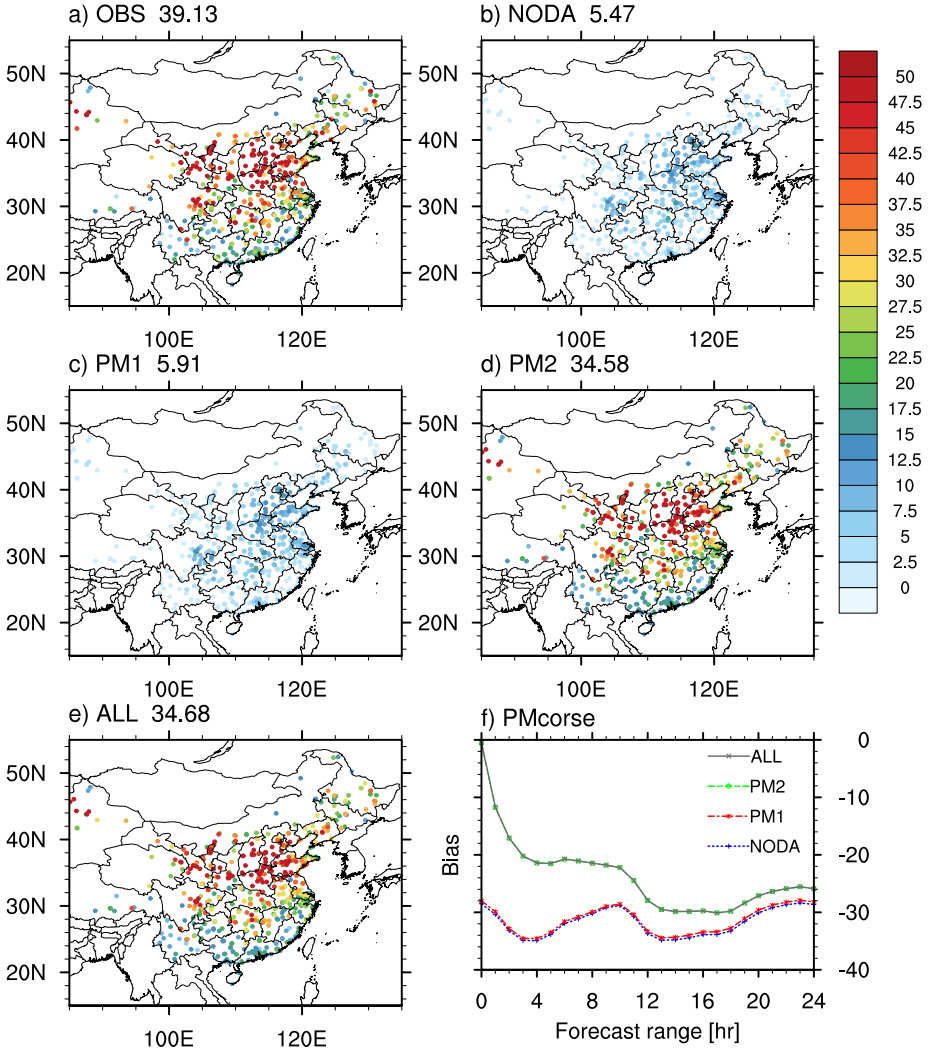


721

722 **Figure 3.** Averaged PMcoarse ($PM_{10-2.5}$, units: μg/m$^3$) at 00 UTC over January 1-31, 2017 in (a)
723 observation and four experiments (b) NODA, (c) PM1, (d) PM2, (e) ALL, and (f) averaged bias (units:
724 μg/m$^3$) for PMcoarse in different experiments as a function of forecast range (the blue, red, green and
725 gray lines denote the results of experiment NODA, PM1, PM2, ALL, respectively), verified against
726 the surface observations of 531 stations in China. The numbers on the top of each panel denote the
727 average PMcoarse concentrations over 531 stations (units: μg/m$^3$).

https://doi.org/10.5194/acp-2019-969
Preprint. Discussion started: 23 January 2020


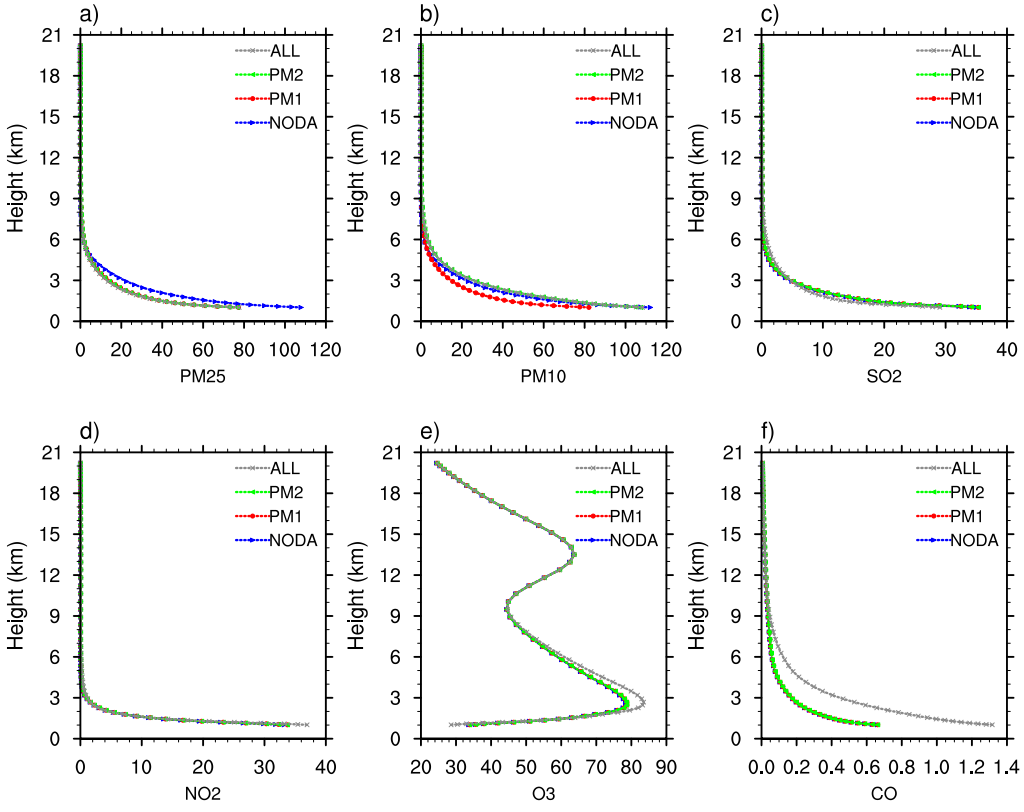


728

729 **Figure 4.** Vertical profile of the analysis at 00 UTC over January 1-31, 2017 for (a) $PM_{2.5}$, (b) $PM_{10}$,
730 (c) $SO_2$, (d) $NO_2$, (e) $O_3$, and (f) CO in different experiments, averaged over the 531 surface stations
731 in China. The blue, red, green and gray lines denote the results of experiment NODA, PM1, PM2, and
732 ALL, respectively. Units of the y-axis are $\mu g/m^3$ in Figs. 4a-e and $mg/m^3$ in Fig. 4f.

https://doi.org/10.5194/acp-2019-969
Preprint. Discussion started: 23 January 2020


Atmospheric Chemistry and Physics Discussions

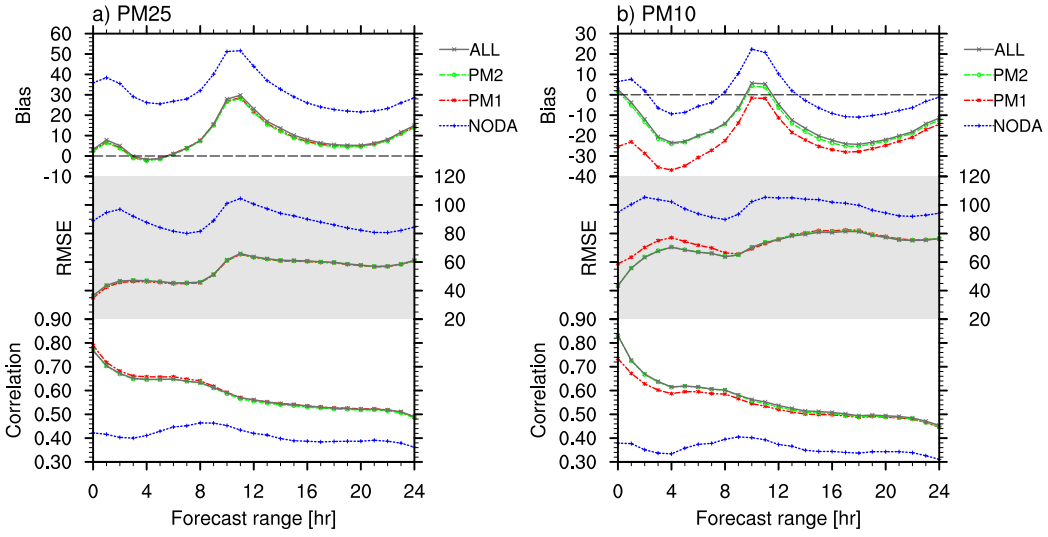


733

734 **Figure 5.** Averaged bias (units: μg/m$^3$), RMSE (units: μg/m$^3$), and correlation for (a) $PM_{2.5}$ and (b)

735 $PM_{10}$ in different experiments as a function of forecast range, verified against the surface observations

736 of 531 stations in China. The blue, red, green and gray lines denote the results of experiment NODA,

737 PM1, PM2, ALL, respectively.

https://doi.org/10.5194/acp-2019-969
Preprint. Discussion started: 23 January 2020


Atmospheric Chemistry and Physics Discussions

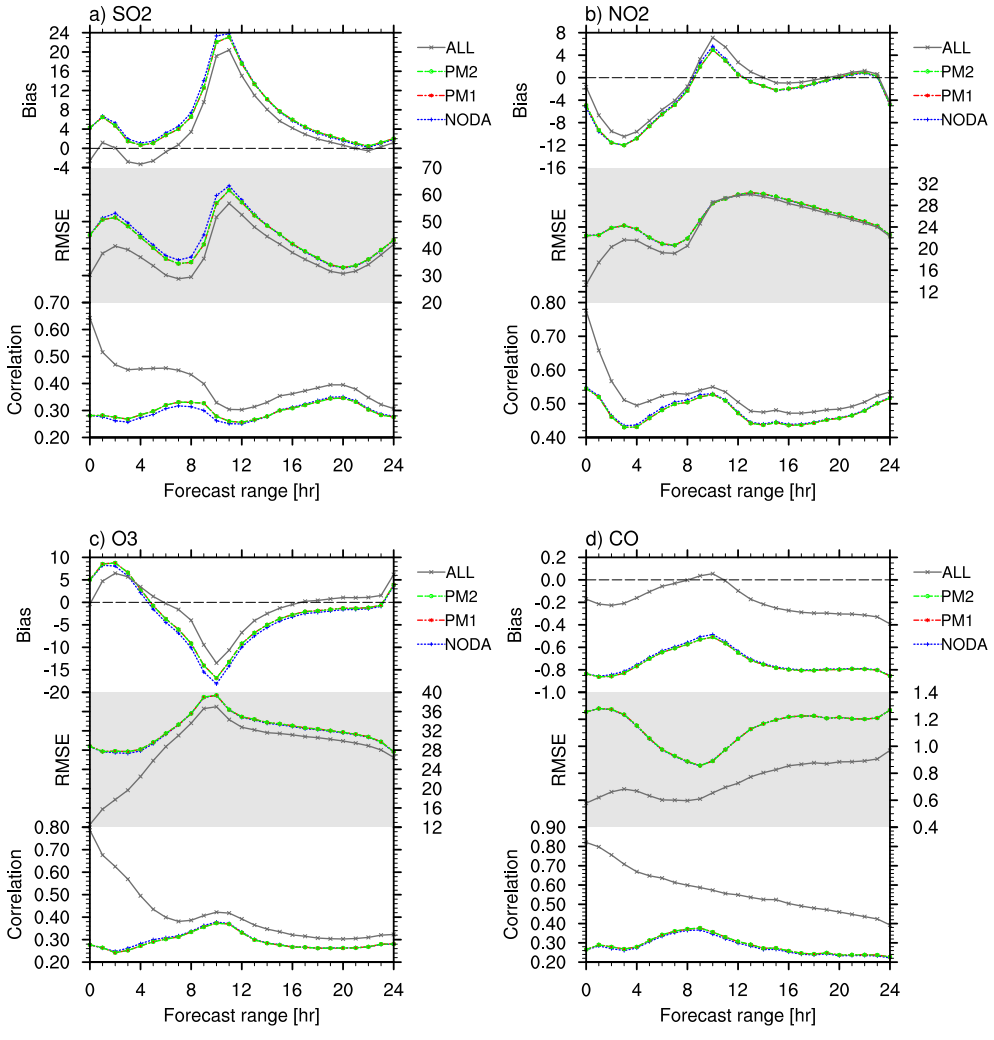


738

739 **Figure 6.** Same as Fig. 5, but for the forecast of (a) $SO_2$, (b) $NO_2$, (c) $O_3$ (units: $\mu g/m^3$), and (d) CO

740 (units: $mg/m^3$).

https://doi.org/10.5194/acp-2019-969
Preprint. Discussion started: 23 January 2020


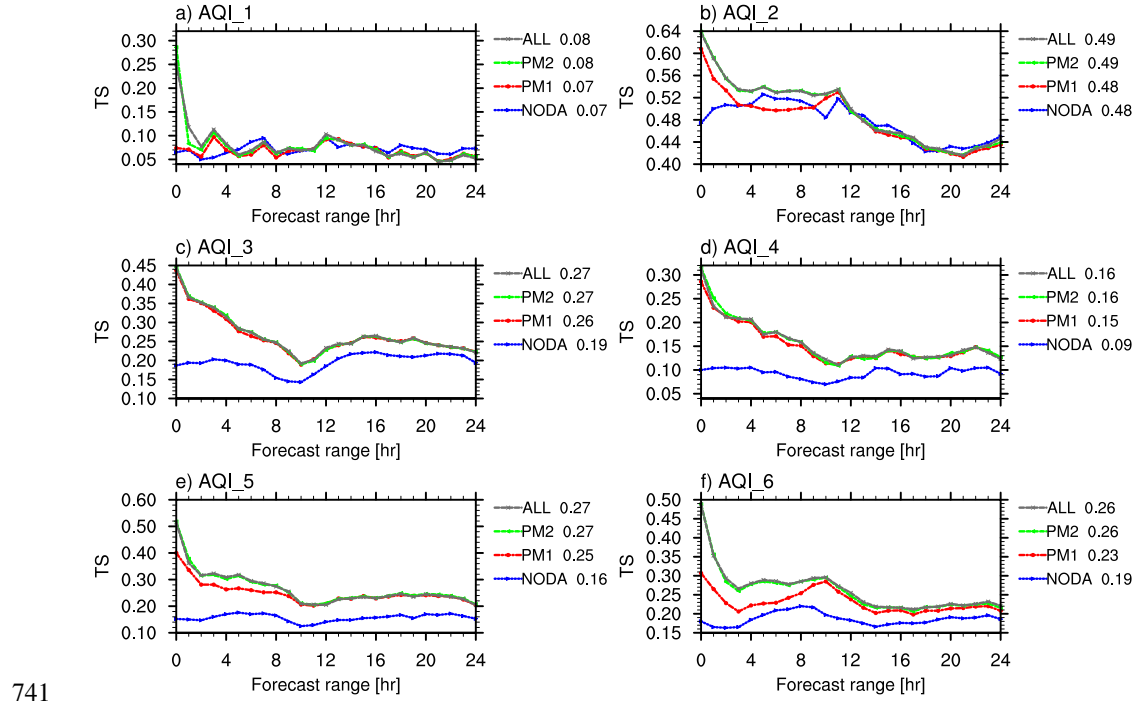


741

742 **Figure 7.** Averaged threat score (TS) for Air Quality Index (AQI) from AQI level 1 to level 6 (a-f) in
743 different experiments as a function of forecast range, verified against the surface observations of 531
744 stations in China. The blue, red, green and gray lines denote the results of experiment NODA, PM1,
745 PM2, and ALL, respectively. The numbers on the right of each panel denote the averaged TS from 0
746 to 24 h for different experiments.

https://doi.org/10.5194/acp-2019-969
Preprint. Discussion started: 23 January 2020


Atmospheric Chemistry and Physics Discussions

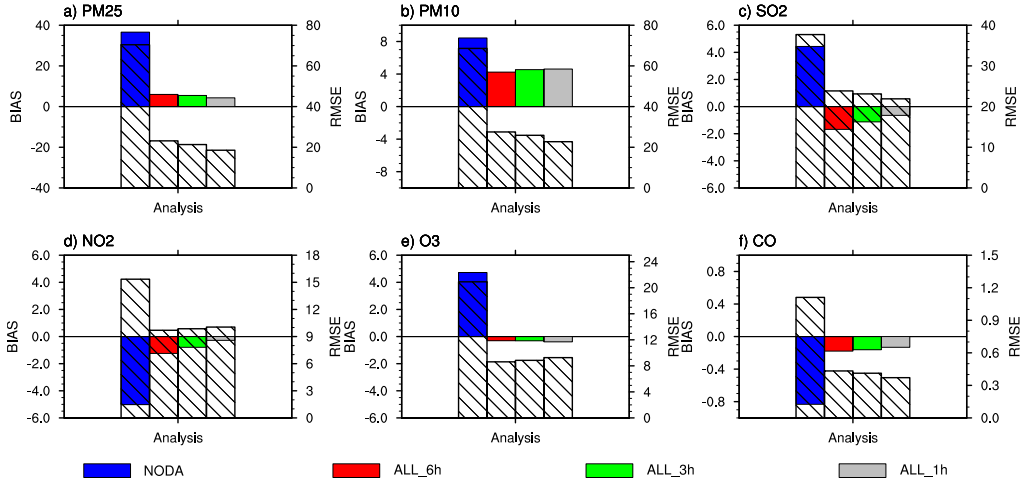


747

748 **Figure 8.** Same as Fig. 2, but for the experiments of NODA, ALL_6h, ALL-3h, ALL_1h, respectively.

749 Units of the y-axis are μg/m$^3$ in Figs. 8a-e and mg/m$^3$ in Fig. 8f.

750

https://doi.org/10.5194/acp-2019-969
Preprint. Discussion started: 23 January 2020


Atmospheric Chemistry and Physics Discussions

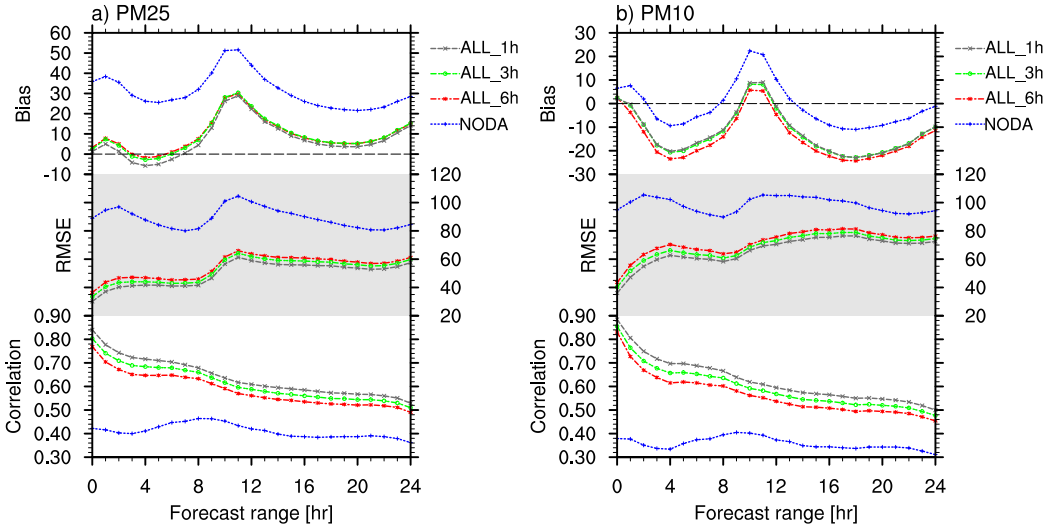


751

752 **Figure 9.** Averaged bias (units: μg/m$^3$), RMSE (units: μg/m$^3$), and correlation for (a) $PM_{2.5}$ and (b)

753 $PM_{10}$ in different experiments as a function of forecast range, verified against the surface observations

754 of 531 stations in China. The blue, red, green and gray lines denote the results of experiment NODA,

755 ALL_6h, ALL_3h, and ALL_1h, respectively.

https://doi.org/10.5194/acp-2019-969
Preprint. Discussion started: 23 January 2020


Atmospheric Chemistry and Physics Discussions

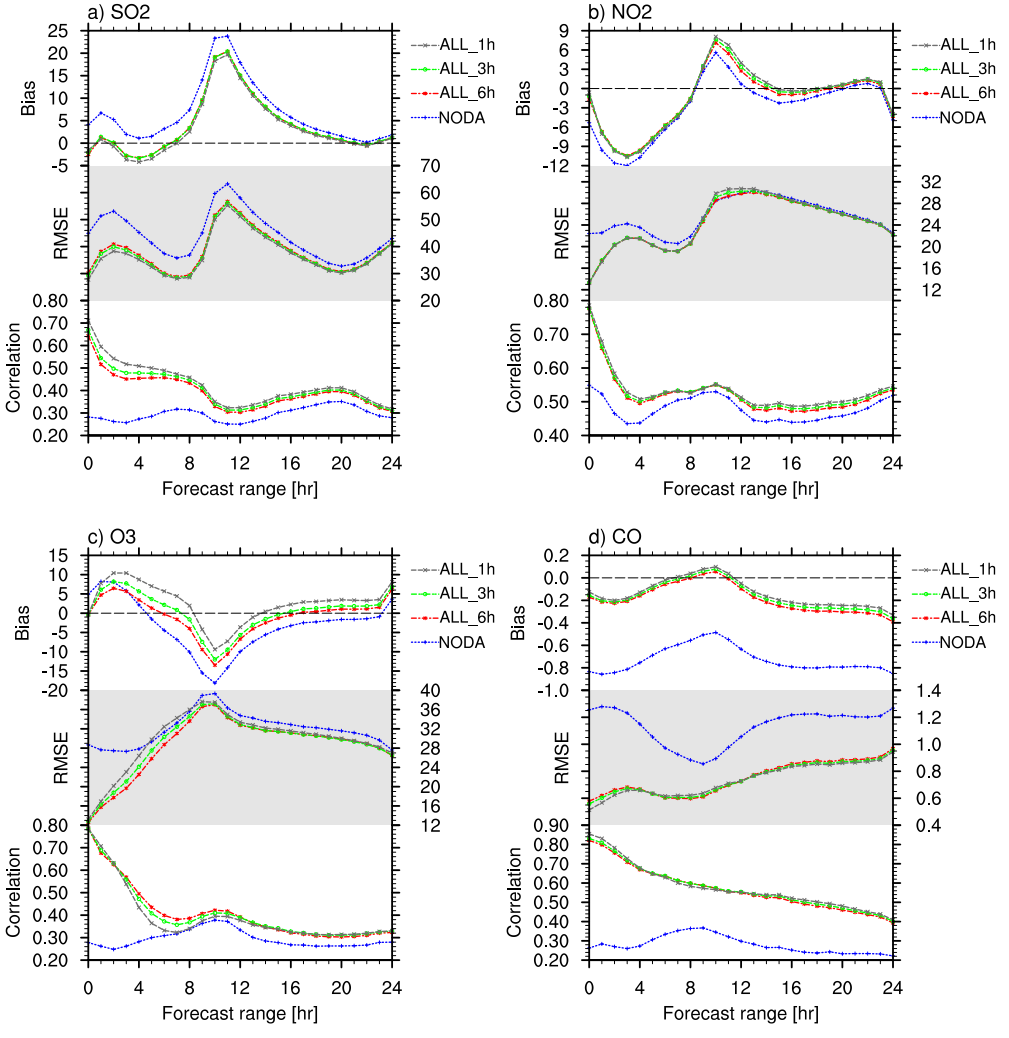


**Figure 10.** Same as Fig. 9, but for the forecast of (a) $SO_2$, (b) $NO_2$, (c) $O_3$ (units: $\mu g/m^3$), and (d) CO (units: $mg/m^3$).

https://doi.org/10.5194/acp-2019-969
Preprint. Discussion started: 23 January 2020


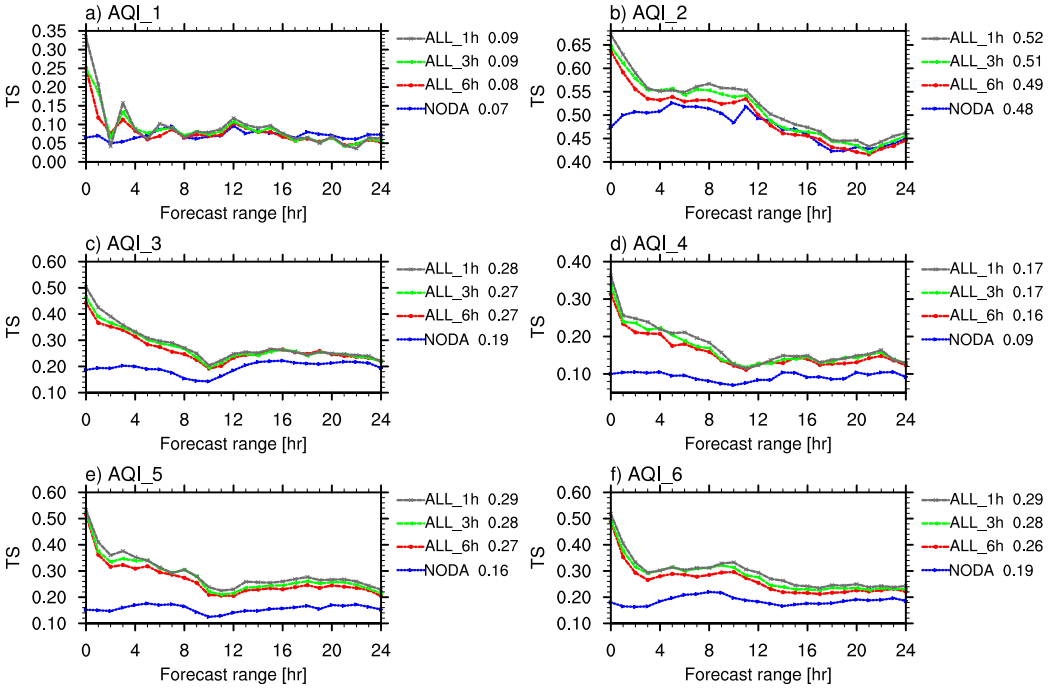


759

760 **Figure 11.** Same as Fig. 7, but for the experiments of NODA, ALL_6h, ALL-3h, ALL_1h, respectively.

https://doi.org/10.5194/acp-2019-969
Preprint. Discussion started: 23 January 2020


Atmospheric Chemistry and Physics Discussions

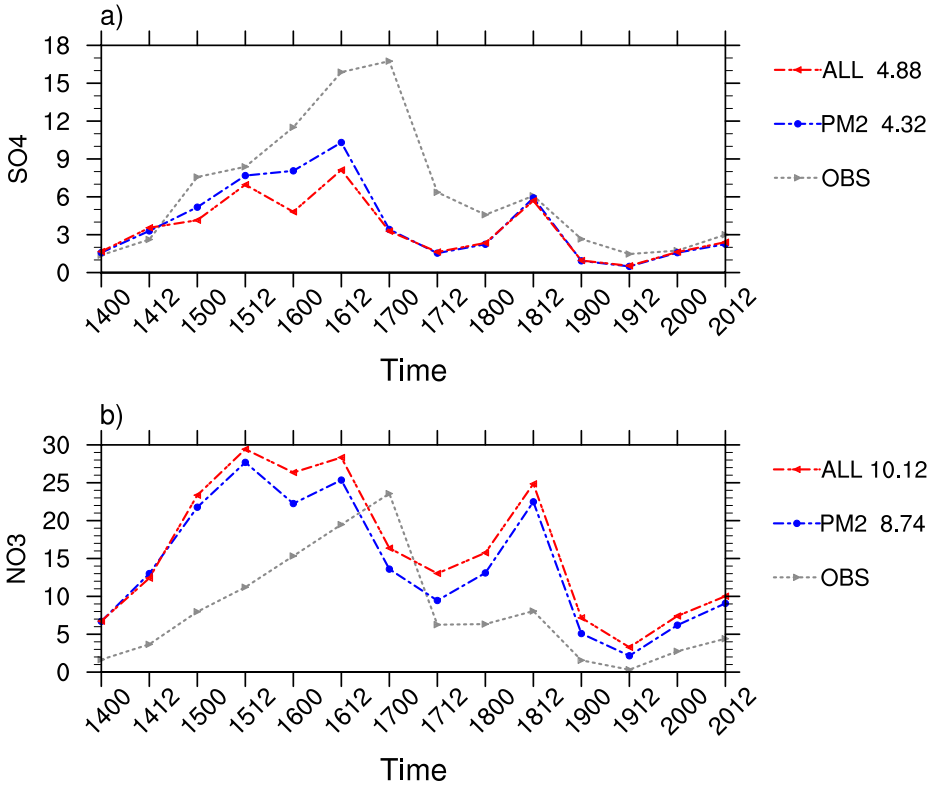


761

762 **Figure 12.** Time series of (a) sulfate, (b) nitrate over January 14-20, verified against the size-resolved
763 particle observation at IUM station. The gray, blue and red lines denote the observation and the results
764 of experiment PM2 and ALL, respectively. The numbers on the right of each panel denote the averaged
765 RMSE over January 14-20 for different experiments.

https://doi.org/10.5194/acp-2019-969
Preprint. Discussion started: 23 January 2020


Atmospheric Chemistry and Physics Discussions

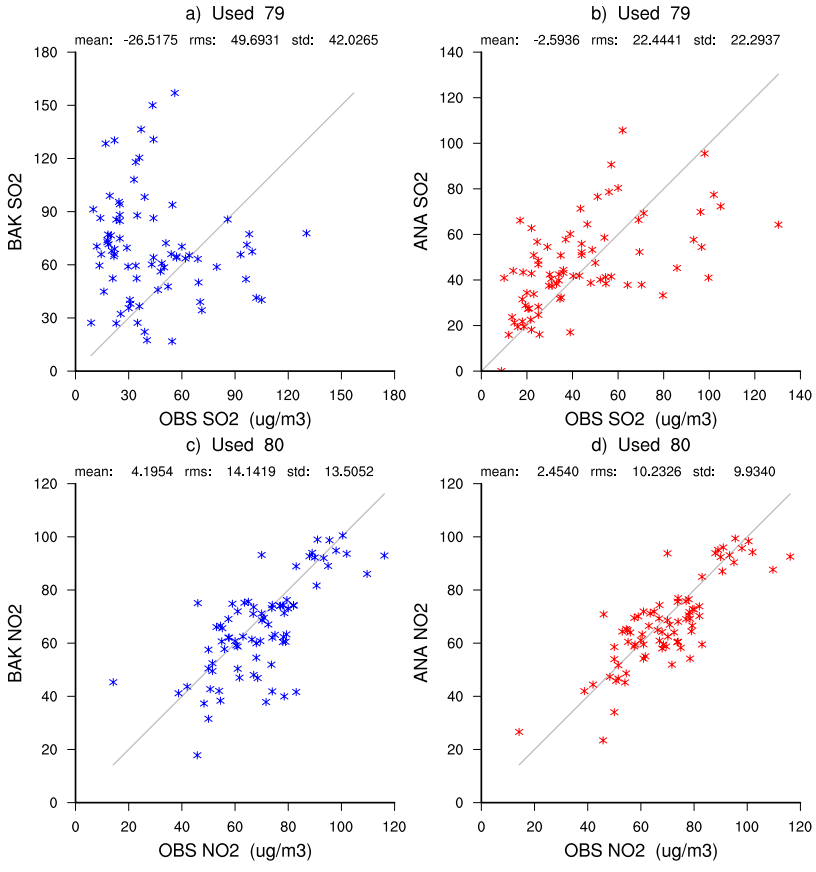


766

767 **Figure 13.** Averaged scatter plot of (a, c) observation versus background and (b, d) observation versus

768 analysis for (a, b) $SO_2$ and (c, d) $NO_2$ around Beijing area (red dots in Fig. 1) on January 16.